Transactions

RRFM 2010

Marrakech, Morocco
21 -25 March 2010

organised in cooperation with:

IAEA
International Atomic Energy Agency
Atoms For Peace

European Nuclear Society
Rue Belliard 65
1040 Brussels, Belgium
Phone + 32 2 505 30 54
Fax +32 2 502 39 02
E-mail ens@euronuclear.org
Internet www.euronuclear.org

ISBN 978-92-95064-10-2

These transactions contain all contributions submitted by 19 March 2010.

Session IV

Innovative Methods in Research Reactor Analysis and Design

NEUTRONICS ANALYSIS OF THE CURRENT CORE OF THE TRIGA MARK II REACTOR VIENNA

R. KHAN, S. KARIMZADEH, H. BÖCK, M. VILLA
Vienna University of Technology
Atominstitute
Stadionallee 2,
A-1020, Vienna, Austria

ABSTRACT

This paper presents the part of PhD work performed at the TRIGA Mark II Vienna. A detailed three dimensional MCNP model of the reactor was developed. The neutronics library JEFF3.1 was applied to this model. The model was completed by employing the fresh fuel composition experiments and was confirmed by the initial criticality, reactivity distribution and thermal flux distribution performed in 1962. To analyse the current burned core, burn up and its relevant material composition was calculated by ORIGEN2 and confirmed by gamma spectroscopy of six spent Fuel Elements FE(s). This new material composition of the current core was incorporated into the already developed MCNP model. This paper presents the current core calculations employing MCNP5 and its experimental validation through criticality and reactivity distribution experiments, performed at the TRIGA Mark II research reactor Vienna. The MCNP predicts the criticality of the current core on loading of 78^{th} FE in the core which is also confirmed experimentally. Five FE(s) were calculated and measured for their reactivity worths. The deviations between theoretical results and experimental observations were in range from 3% to 17%.

1. Introduction

The Atominstitute Vienna operates a TRIGA Mark II research reactor since March 1962 at a nominal power of 250 kW, used for research and training needs in nuclear technology. The reactor is further utilized in the fields of fields of neutron, solid state physics, reactor safety, radiochemistry, radiation protection, dosimetry and low temperature physics. It employs a unique Uranium-Zirconium-Hydride (U-ZrH) fuel which is a homogeneous mixture of uranium and zirconium hydride. Hydrogen is incorporated into the fuel by mixing uranium with zirconium hydride. Most of the moderation of the fast fission neutrons in TRIGA reactors is due to this hydrogen, which is at the fuel temperature level, rather than at the coolant temperature level. The U-ZrH fuel also allows pulse operation of the TRIGA up to 250 MW for 40 milliseconds. Any power excursion is reduced automatically within milliseconds, faster than any engineered device can operate. Because of its inherent safety, no special containment or confinement building is required.

The reactor core is a cylindrical lattice in which Fuel Elements FE(s), 3 Control Rods CR(s), Graphite Elements GE(s), Source Element (SE) and two pneumatic systems are arranged into five circular rings (B, C, D, E and F) around the central thimble A. For each fuel element, the fuel meat is sandwiched between two graphite end sections that form the top and bottom reflector. An annular graphite radial reflector surrounds the core and is supported on an aluminum stand at the bottom of the tank [1].

An extensive and versatile core of the reactor is visible through vertical water shield. The reactor is equipped with many experimental facilities inside and outside the reactor core. Outside the core, there is annular grooved graphite reflector, four beam tubes, thermal column, and graphite collimator while inside the core; there are about 17 irradiation holes to measure the radial and axial flux in the core which also include the central channel names as ZBR. The top and side view of the reactor can be seen in Figure 1.

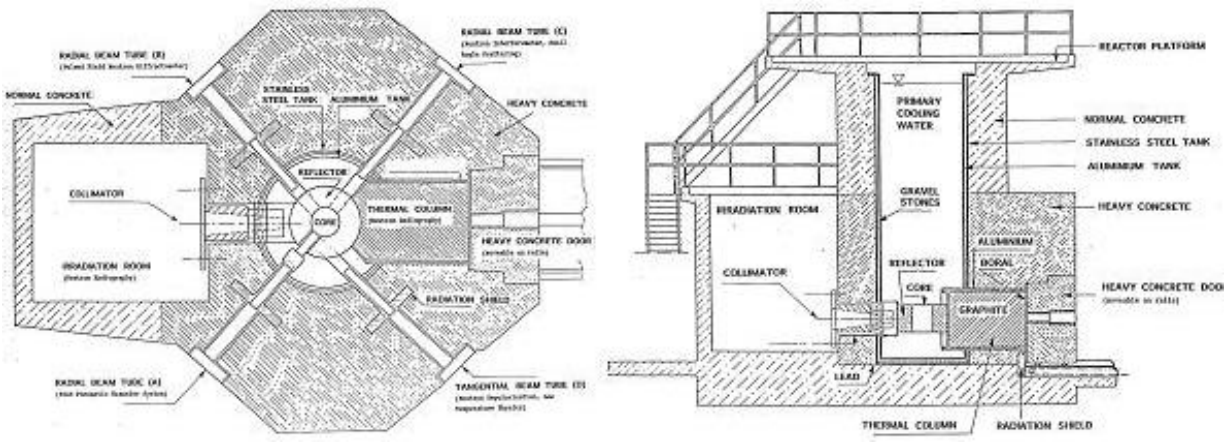

Fig 1. Top (left) and side (right) views of the TRIGA Mark II research reactor, Vienna [1].

The current TRIGA core is a mixed core of three different types of FE(s) i.e. aluminium clad (or 102 type), stainless steel clad (or 104 type) and FLIP (or 110 type) FE(s). Bothe 102 and 104 types of fuel are 20% enriched while the FLIP (Fuel Life Improvement Program) fuel uses 70% enriched uranium with a stainless steel cladding. The current core loading is 83 FE(s) with 54 elements of 102 type, 20 FE(s) of 104 type and remaining 9 FE(s) are FLIP FE(s) [1] and is shown in Figure 2 [2].

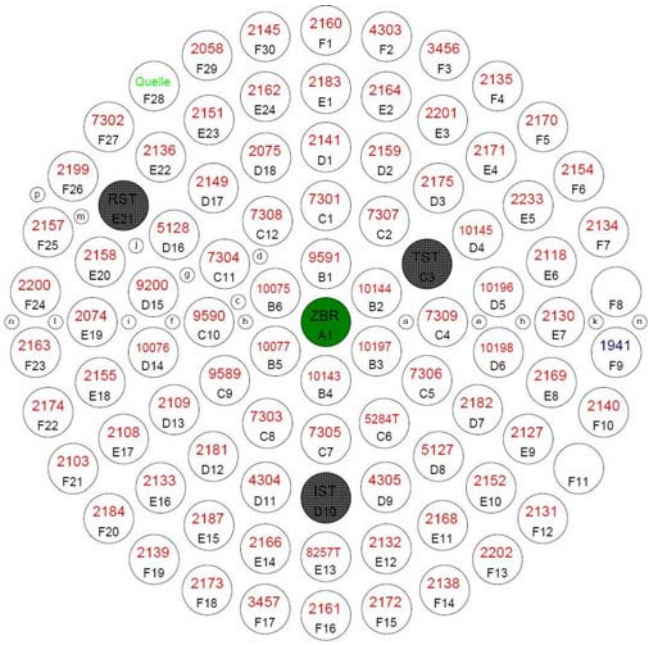

Fig 2. The current core map of the TRIGA Mark II Vienna, research reactor.

2. MCNP Model

The MCNP model, based on the fresh fuel composition, was modified into the current core model. The current core model incorporates the burned fuel material composition. This burned fuel material composition was calculated by ORIGEN2 and confirmed by gamma scanning of six spent fuel elements [2]. This model includes the core components (FE (s), CR(s), GE, SE etc), four beam tubes, thermal and thermalising column. The MCNP model of the current core is shown in Figure 3. In this model, all 83 FE(s) were divided into 15 groups on the basis of their burn-ups. Therefore MCNP assigns different colour to each burn-up group [3].

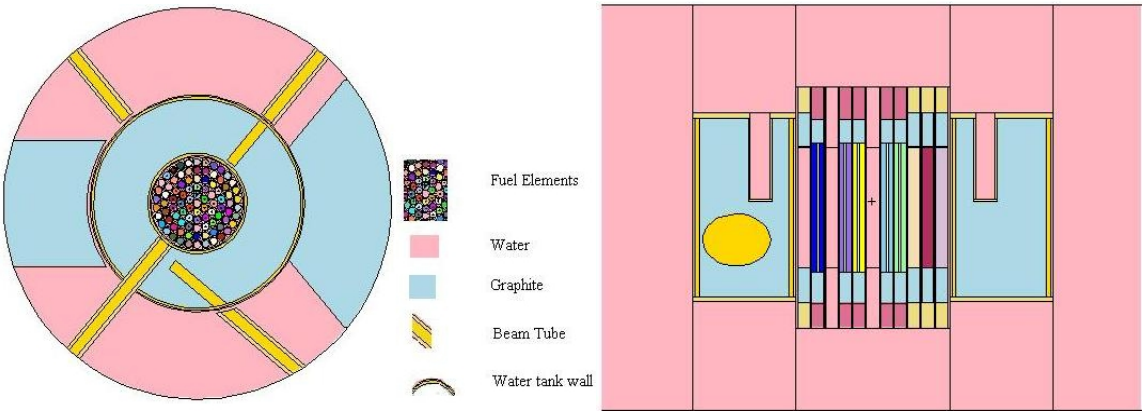

Fig 3. Top (left) and side (right) views of the MCNP model of TRIGA Mark II research reactor.

3. MCNP Model Validation

Criticality Experiment:
To perform this experiment, 10 FE(s), 2 from each ring B, C, D, E and F, were removed from the core and placed into the in-tank storage positions. The fuel elements were added to the core one by one starting from the B ring outward. After the addition of each fuel rod, the signal (counts per second) from a fission chamber indicated the increase in the reactivity. The same experimental conditions were applied to MCNP model and calculated the effective multiplication factor K-eff of the core after each FE insertion

The experimental observations and its MCNP calculations are shown in Figure 4. The S73d (or S73u) represents the neutron count rate when 73 FE(s) are in the core with all three CR(s) in fully down (or fully up positions) respectively. Similarly the symbol Sxxd (or Sxxu) is used for neutron count rate after each addition of FE. The ratios (Sxxd/S73d and Sxxu/S73u), after each addition of FE, were calculated.

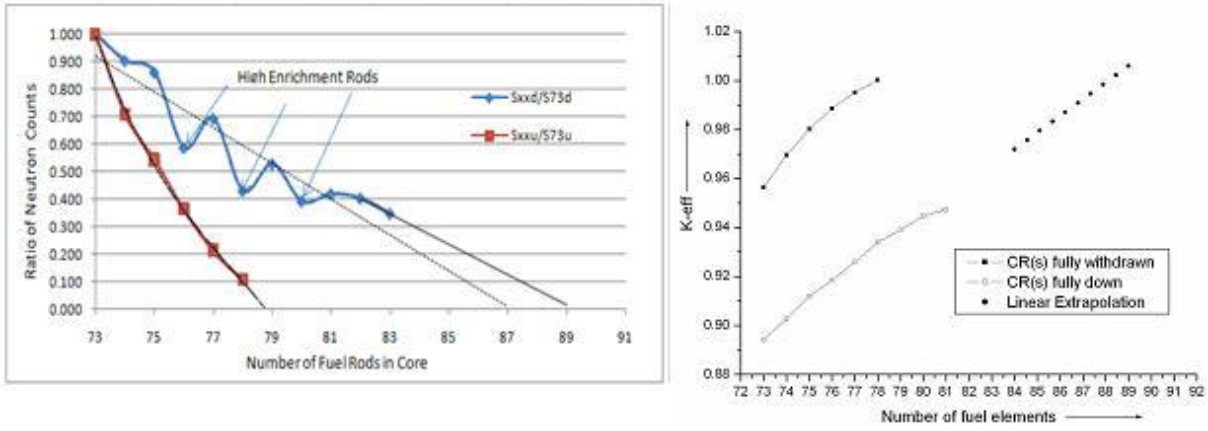

Fig 4. The experimental (left) and theoretical (right) results of the reactivity distribution experiment of TRIGA Mark II reactor core.

Reactivity Distribution Experiment:
Keeping the burn-up group approximation and control rod effects into consideration, the five FE(s), 10077(in B05), 10198(in D05), 7301(in C01), 2133 (in E16) and 2184(inF20), were selected for this experiment. Using the shim rod calibration performed on 29 June 2009, a reactivity worth measurement of these FE(s) was performed. This reactivity distribution experiment was performed at the core configuration of Figure 2, where each removed fuel element was replaced by water during its measurement. The reactivity difference between the

two positions of shim rod provides the reactivity worth of the measured FE. The same experimental procedures were applied to MCNP current core model to calculate the reactivity worth of each FE. The tabular and graphical comparison of measurements and calculations are given in Table 1 and Figure 5.

Sr. No.	FE No.	Exp. reactivity worth(cents)	Theo. Reactivity worth (cents)	%-difference
1	10077	1.29	1.48	12.8
2	7301	0.80	0.67	17.5
3	10198	0.58	0.56	3.4
4	2133	0.48	0.50	4.0
5	2184	0.27	0.26	3.7

Tab 1: Comparison between measurements and calculations of reactivity worths of FE

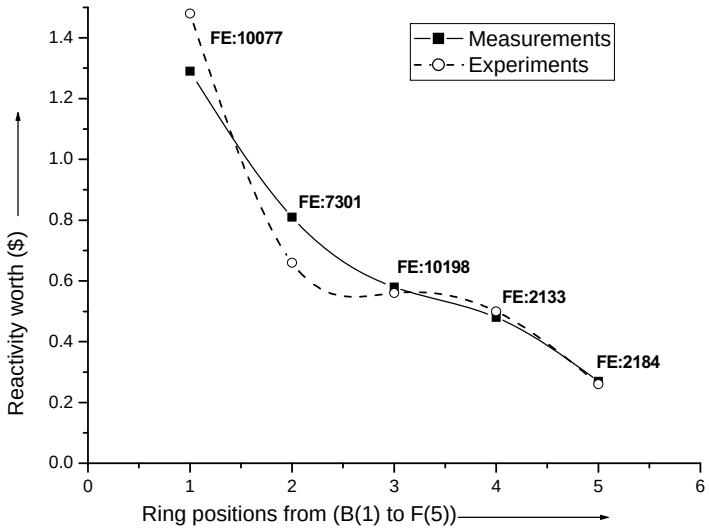

Fig 5. Calculated and measured reactivity worth of 5 FE(s)

4. Results and Discussions

Criticality Experiment:

In case of all three CR(s) in the fully up positions, MCNP predicts the criticality of the current core with the 78th FE (2109 in D13 position) loading to the core as shown in Figure 4 (right). The simulation gives the value of 1.31 cents as positive reactivity upon loading of FE no. 2109. Experimentally, the brown line, when extrapolated in figure 4 (left side) indicates that the current core reaches criticality after the insertion of 78th FE (2019) with all CR(s) in completely up positions. This brown curve confirms the positive reactivity insertion as it intersects the line just before addition of 79th FE. But this line does not give the reactivity value due to experimental limitations. Figure 4 shows good agreement between MCNP predictions and experimental observations.

In case of all three CR(s) in the fully down positions, both experimental and theoretical results show the difference in reactivity values for each added FE as given in Figure 4. This may be because each FE has different fissile material composition and hence has a different effect on core reactivity. The measurements confirm the calculations that the core does not

achieve its criticality on addition of all 83 FE(s) when CR(s) are kept fully out. This is due to the shut down margin of CR(s). If the linear fit of the experimental data points (Figure 4(left)) is extrapolated, the core may become critical on addition of FE(s) from 87 to 89 depending on the initial point of the extrapolation. In case of MCNP results, when a linear fit of the theoretical data point is extrapolated, the core will become critical on addition of 88th FE in the core assuming that each additional fuel rod will increase the reactivity of the core according to the average trend.

Reactivity Distribution Experiment:
Table 1 and Figure 5 show the comparison of the theoretical and experimental results of the reactivity distribution experiment. This experiment was performed with the current core configuration as given in Figure 2. Generally, the MCNP results look consistent with the experimental results. The calculations are closer to experimental results in outer ring positions (i.e. D, E and F) than inner ring positions (i.e. B and C-ring) of the core. It may be due to, when FE is inserted into the core, more severe local flux distribution is deformed in inner rings than outer rings [4]. The other possible reason of these deviations could be the fact that the calculations were performed with fixed control rod positions while, in the experiment, the control rod positions were re-adjusted for each measurement of FE.

5. Conclusion and outlook

The already developed MCNP model employing fresh fuel composition was modified for the current core. The current core model contains 83 FE(s) and incorporates the burned fuel composition. This model was executed for criticality and reactivity distribution experiments. To verify these calculations, both criticality and reactivity distribution experiments were performed at TRIGA Mark II research reactor. The calculations and measurements were found in good agreement. This model can be applied to calculate the current core parameters like feedback reactivity coefficients, effective delayed neutron fraction and radial and axial flux distribution of the core.

6. References

1. General Atomic (GA), March 1964. TRIGA Mark II Reactor General Specifications and Description. General Atomic Company, U.S.A.
2. R. Khan, S. Karimzadeh, H. Boeck, 2009. TRIGA fuel Burn up calculations supported by gamma scanning. RRFM 2009, Vienna, Austria.
3. Monte Carlo Team, “MCNP – A General Monte Carlo N-Particle Transport Code, Version 5”, LA-UR-03-1987, Los Alamos National Laboratory, April 24, 2003.
4. Tetsuo Matsumoto and Nobuhro Hayakawa, Dec. 2000, Benchmark Analysis of TRIGA Mark II Reactivity Experiment using a Continuous Energy Monte Carlo Code MCNP, Nuclear Science and Technology, vol. 37, no. 12, p. 1082-1087.
5. James J. Duderstadt and Louis J. Hamilton, 1976, “Nuclear Reactor Analysis”, John Wiley and Sons, New York.

APPLICATION OF RELAP/SCDAPSIM WITH INTEGRATED UNCERTAINTY OPTIONS TO RESEARCH REACTOR SYSTEMS THERMAL HYDRAULIC ANALYSIS

C. M. ALLISON, J. K. HOHORST
Innovative Systems Software, LLC
Idaho Falls, Idaho 83404 USA
iss@relap.com

M. PEREZ, F. REVENTOS
Technical University of Catalonia
Avda. Diagonal 647
08028 Barcelona, SPAIN
marina.perez@upc.edu, francesc.reventos@upc.edu

ABSTRACT

The RELAP/SCDAPSIM/MOD4.0 code, designed to predict the behavior of reactor systems during normal and accident conditions, is being developed as part of the international SCDAP Development and Training Program (SDTP). RELAP/SCDAPSIM/MOD4.0, which is the first version of RELAP5 completely rewritten to FORTRAN 90/95/2000 standards, uses publicly available RELAP5 and SCDAP models in combination with advanced programming and numerical techniques and other SDTP-member modeling/user options. One such member developed option is an integrated uncertainty analysis package being developed jointly by the Technical University of Catalonia (UPC) and Innovative Systems Software (ISS). This paper briefly summarizes the features of RELAP/SCDAPSIM/MOD4.0 and the integrated uncertainty analysis package, and then presents an example of how the integrated uncertainty package can be setup and used for a simple pipe flow problem.

1. Introduction

RELAP/SCDAPSIM[1-3], designed to predict the behavior of reactor systems during normal and accident conditions, is being developed at Innovative Systems Software (ISS) as part of the international SCDAP Development and Training Program (SDTP)[4,5]. RELAP/SCDAPSIM uses the publicly available SCDAP/RELAP5[6,7] models developed by the US Nuclear Regulatory Commission in combination with proprietary (a) advanced programming and numerical methods, (b) user options, and (c) models developed by ISS and other SDTP members. RELAP/SCDAPSIM/MOD4.0[3], the latest in the series of SDTP-developed versions, is the first version of RELAP5 or SCDAP/RELAP5 completely rewritten to FORTRAN 90/95/2000 standards. MOD4.0 is described briefly in Section 2.0.

The RELAP/SCDAPSIM/MOD4.0 integrated uncertainty package[8,9] provides the end user with a “user-friendly” best estimate system thermal hydraulic and severe accident analysis code that be used as part of a formal uncertainty analysis methodology or simply as a convenient way to determine the influence of key physical phenomena or user defined input quantities on calculational results. The integrated package is being developed jointly by the Technical University of Catalonia (UPC) and Innovative Systems Software (ISS). The uncertainty package is described in Section 3.0.

The integrated package can be applied to any standard RELAP5 or RELAP/SCDAPSIM input model. The user simply defines the code parameters that are considered to be influential in the calculations, defines their associated uncertainty distributions, and the desired output quantities with uncertainty bands. The code then uses the original input model along with the

uncertainty input to generate the desired results. An example describing the application of the package to flow in a pipe is discussed in Section 4.0.

2. RELAP/SCDAPSIM

RELAP/SCDAPSIM is designed to describe the overall reactor coolant system (RCS) thermal hydraulic response and core behavior under normal operating conditions or under design basis or severe accident conditions. The RELAP5 models calculate the overall RCS thermal hydraulic response, control system behavior, reactor kinetics, and the behavior of special reactor system components such as valves and pumps. The SCDAP models calculate the behavior of the core and vessel structures under normal and accident conditions. The SCDAP portion of the code includes user-selectable reactor component models for LWR fuel rods, Ag-In-Cd and B4C control rods, BWR control blade/channel boxes, and general core and vessel structures. The SCDAP portion of the code also includes models to treat the later stages of a severe accident including debris and molten pool formation, debris/vessel interactions, and the structural failure (creep rupture) of vessel structures. The latter models are automatically invoked by the code as the damage in the core and vessel progresses.

As described in more detail in reference 3, RELAP/SCDAPSIM/MOD4.0 has been completely rewritten to FORTRAN 90/95/2000 standards. This work took 3 years to complete and involved the rewriting of more than 300,000 lines of coding but resulted in dramatic improvements in the ability to maintain and improve the code. MOD4.0 also includes advanced numerical options and coding that allows the code to run reliably at faster-than-real time for complex plant models. In addition to the integrated uncertainty analysis option, MOD4.0 also is used with standardized interfaces for other coupled calculations such as 3D reactor kinetics[10] and plant simulation and training Graphical User Interfaces[11-13].

3. Integrated Uncertainty Analysis Package

RELAP/SCDAPSIM/MOD4.0 with the integrated uncertainty analysis package can play an important role as part of a formal uncertainty analysis methodology, sometimes called a BEPU (Best Estimate Plus Uncertainty) methodology. This methodology is often used in licensing applications. In such a formal setting, as described in more detail in reference 8, a typical methodology might involve the following steps.

a) Selection of the plant.
b) Selection of the scenario.
c) Selection of the safety criteria.
d) Identification and ranking of the relevant phenomena based on the safety criteria.
e) Selection of the appropriate code parameters to represent those phenomena.
f) Definition of the Probability Density Functions (PDFs) for each selected parameter.
g) Performing a number of computer runs with a random sampling of the selected parameters according to its PDF.
h) Processing the results of the multiple computer runs to estimate the uncertainty bands for the computed quantities associated with the selected safety criteria.

In this setting, the base input model for RELAP/SCDAPSIM would define the plant and scenario while the code models and correlations, in conjunction with the user selected modeling options, would describe the relevant phenomena. The uncertainty package then allows the user to (a) select the code parameters, i.e. important correlations, and associated input modeling options, (b) define the relevant PDFs, (c) define the number of random samples, and (d) select desired computed quantities with associated uncertainty bands. The user can further analyze the results to determine the influence of individual code parameters on the desired computed quantities.

The integrated code also provides a convenient way to perform sensitivity analyses with any input model. The process is the same as the proceeding methodology except identification of the important code parameters and relevant PDFs may be done in an informal way and the ranking of the relative importance of the code parameters determined from the analysis of the uncertainty results.

The use of the uncertainty package involves three phases or three user options. The first phase or option is the setup phase. The setup phase involves a single RELAP/SCDAPSIM run with the setup option selected. The setup options allows the user to identify

a) The number of uncertainty runs needed.
b) Source code parameters and associated PDFs
c) Input parameters and associated PDFs.

The number of code runs can either be computed by the code or be fixed by the user. In the former case, the code uses the Wilks[14,15] formula to determine the appropriate runs. The user can continue a previous set of runs or eliminate runs without starting a new process. The package also includes the possibility of adding extra runs, setting a maximum or minimum number of runs, and the introduction of the seed to start the random generating process.

The uncertainty parameters that can be selected by the user can either be source code or input parameters. The source code parameters allow the user to perturb computed quantities not normally accessible through input. For example, source code parameters include:

- *Interfacial heat transfer coefficients.*
- *Heat transfer coefficients.*
- *Critical Heat Flux.*
- *Gap thermal conductivity from the gap conductance model.*
- *Viscosity.*
- *Thermal conductivity.*
- *Surface tension.*

The input parameters, as the name implies, are parameters that are defined through the input model. Examples might be boundary conditions, loss coefficients, etc. The package allows the user to easily perturb any input quantity by specifying the location in the input file (card and word number).

The user can select from a variety of PDFs and then specify the associated characteristic parameters for each parameter to be perturbed. For instance when a Normal Distribution is desired, the user must specify the mean and the standard deviation. Four types of PDFs can be selected:

- *Normal distribution.*
- *Uniform distribution.*
- *Log-normal distribution.*
- *Trapezoidal distribution.*

The second phase is the simulation phase. This phase uses the results from the setup phase as well as the base input model to perform all of the desired runs. Since these runs only require the base input model and output files generated in the setup phase, these runs can be performed sequentially on a single machine (typical of most transients and models) or distributed to different machines or CPUs for transients that might involve hours of problem time. For example, transients involving loss of offsite power and the slow heat up of the reactor tank may take hours to evolve.

The last phase, post-processing phase, uses data coming from previous phases to build the uncertainty bands for the requested uncertainty output quantities. At the conclusion of the post-processing run, the code will automatically produce time dependent graphs for each requested output quantities including:

- *Upper and lower uncertainty bands.*
- *Base case value.*
- *Difference between upper and lower values at each time step.*

The post-processing phase also generates an EXCEL compatible file with the sorted values for each required quantity in the input file. From these files, scalar quantities such as time of core quench or peak cladding temperature can be obtained with little effort.

4. Example – Application to Flow in a Simple Pipe

The problem that will be analyzed is a very simple one, the flow of water down a vertical pipe as shown in the nodalization diagram given in Figure 1. However, the approach used will be the same as one used when modeling a full reactor system or a component of the reactor system.

The pipe is arbitrarily divided into five axial fluid volumes with flow resulting from a pressure difference and gravity. The flow will be initially set to zero and the problem will run until equilibrium flow and temperature conditions are reached in the fluid and pipe wall. The water coming into the top of the pipe has a temperature of 322 K. The temperature of the water in the pipe is initially set at 305 K. The wall has an initial temperature of 283 K and has an adiabatic boundary condition on the outside. The pressure at the inlet of the pipe is 1.03 MPa with outlet pressure maintained at 0.34 MPa.

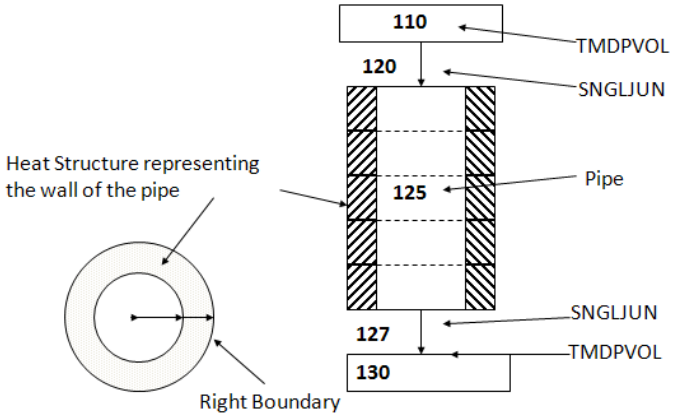

Figure 1 – Nodalization of simple pipe

The temperature of the inner surface of the pipe is shown in Figure 2. The mass flow through the pipe is shown in Figure 3. The heat transfer coefficients on the inner surface of the pipe are shown in Figure 4. These results show a brief period at the beginning of the calculations where there is an initial transient as the stagnant water starts responding to the pressure boundary conditions and gravity. The temperatures at the inner surface show that the inner pipe wall surface temperatures also quickly approach equilibrium as the heat transfer to the fluid moves to a constant value. Although the flows reach equilibrium rather quickly, the wall temperatures take longer as the pipe wall heats. The total time to reach total thermal equilibrium is approximately 200 s so the conditions are still changing slightly at 10 s when the calculations are terminated.

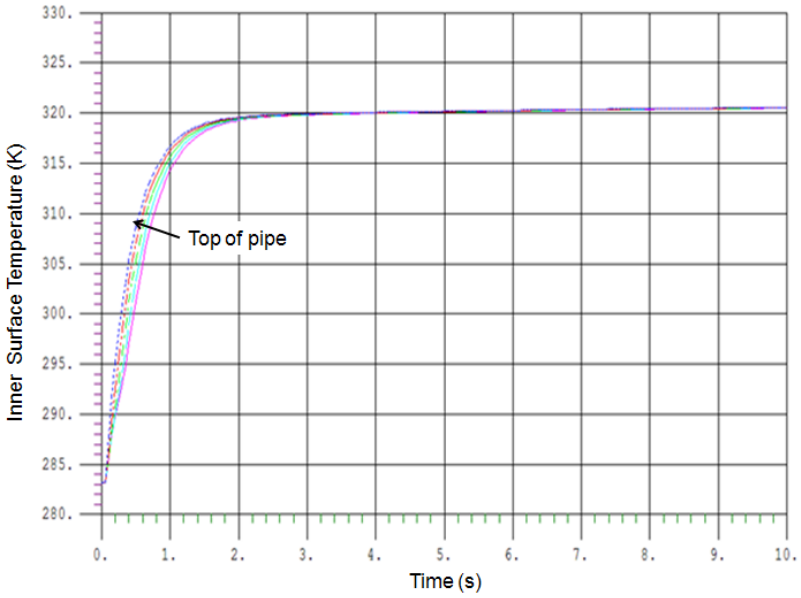

Figure 2 – Temperature of the inner surface of the pipe wall

For the purposes of this example, a combination of source and input parameters is selected for the uncertainty analysis:

- Source parameters
  - Liquid heat transfer coefficient ± 20%
  - Liquid heat transfer viscosity ± 2%
  - Liquid heat transfer thermal conductivity ± 2%
- Input parameters
  - Source pressure ± 20%
  - Inlet junction area ± 20%

The resulting RELAP5 input is shown in Table 1. The first line in the input, starting with the **=**, is the title of the input. The lines starting with ***** are comments. The line starting with **100** is a command line selecting the uncertainty setup option. The lines starting with **290** and **291** are defining the source and then input parameters respectively.

The source input, lines starting with **290**, defines the parameter, such as **HTC** for heat transfer coefficient, the range of heat structures where the heat transfer coefficients are to be perturbed, and the PDF type and characteristics. In this case, the Normal Distribution (**ND**) option is selected with characteristics of the mean and standard deviation input. In the **HTC** example, the user can also select the type of heat transfer coefficient, or convective heat transfer regime, to be perturbed. In this example, since the problem only has heat transfer to a liquid, a single heat transfer regime is perturbed. In the most general of cases, all of the heat transfer regimes that might occur can be explicitly identified. The input parameter input, the lines starting with **291**, the pressure in source volume **110** and the junction flow area in junction **120** are to be perturbed. For example, the pressure in source volume is actually identified by the line number, **1100201**, and word number, **2**, in the base input model. The setup run will then automatically generate all of the files necessary to perform the uncertainty analysis using a number of runs specified by the Wilks formula for a 95% confidence interval. After the necessary runs are completed, a post-processing run is made that generates the results shown in Figures 5 and 6.

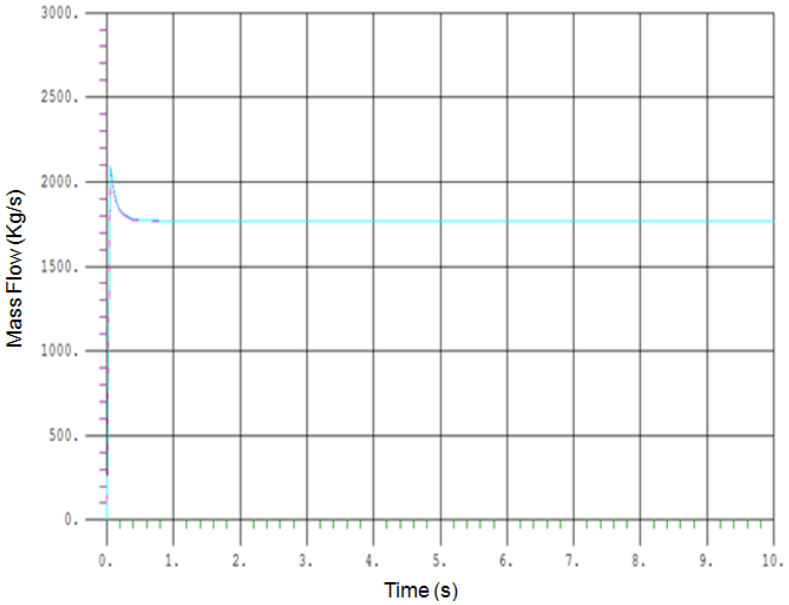

Figure 3 – Mass flow through pipe

Figure 5 shows the results of the uncertainty analysis on the inner surface temperature at the top of the pipe. The pink curve shows the base case result, also shown in Figure 2, with upper and lower bounds for a variation in all of the source and input parameters over their range of uncertainties. The red curve represents the variation between the upper and lower bound. As expected, there is a larger variation in the first second as the flow is accelerating and the heat transfer coefficients are varying noticeably with time as shown in Figure 4. Further analysis of the results would indicate that the most influential uncertainty parameter in the first second is the variation in heat transfer coefficient. Figure 6 shows the results for the mass flow. In this case, the variation is much more significant. Sensitivity analysis, as expected, shows that the variations in source pressure and inlet junction area are the most influential in determining the uncertainty in the mass flow through the pipe.

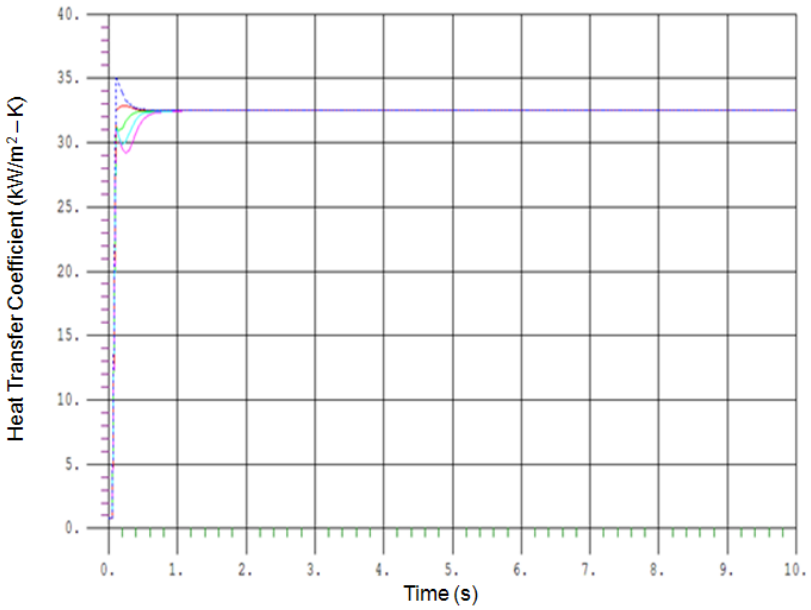

Figure 4 – Heat transfer coefficients on the inside of the pipe wall

```
= Setup of uncertainty option for simple pipe
100 uncsetup
*Defaults to use Wilk's formula application with 95% confidence with order 1
*Defaults for min/max number of runs and initial seed for random sampling
29000000 0 0 0.95 0.95 1
*      Source coef dist. mean std              wt no.
29000001 HTC.02.101 ND 1.0  0.10 0.00 0.00 -1.0  0.0 *Heat transfer coef.
29000002 VIS.LW.LIQ ND 1.00 0.02 0.00 0.00 -1.0 0.0   *Liquid viscosity
29000003 CON.LW.LIQ ND 1.00 0.02 0.00 0.00 -1.0 0.0 *Liquid thermal cond.
29101000 ND 1.0 0.2 0.0  0.0
*                    Source pressure       Junction  area
29101001  -1.0 20 1100201 2 2 1 -1.0 20 1200101 3 3 1 *Input parameters
*Base input deck
*100 new  transnt
.
.
```

Table 1 Input added to RELAP5 base input model to set up the uncertainty analysis

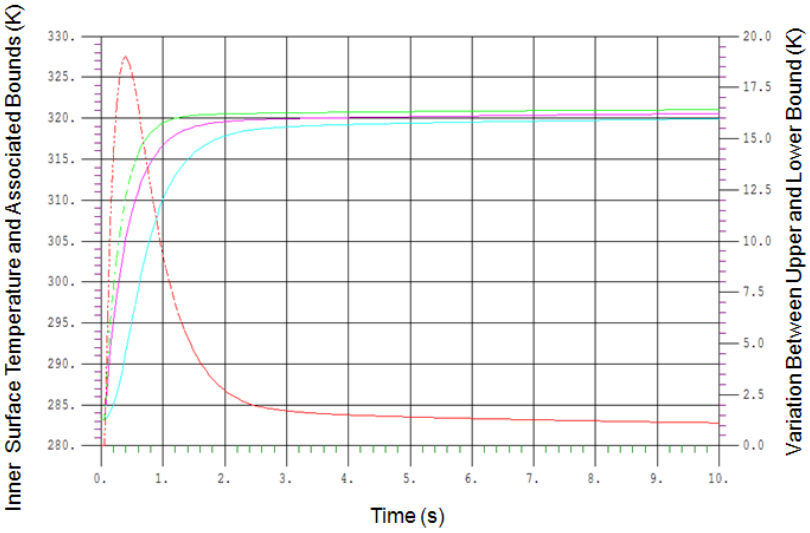

Figure 5 – Inner pipe wall temperature at top of pipe with associated uncertainty limits

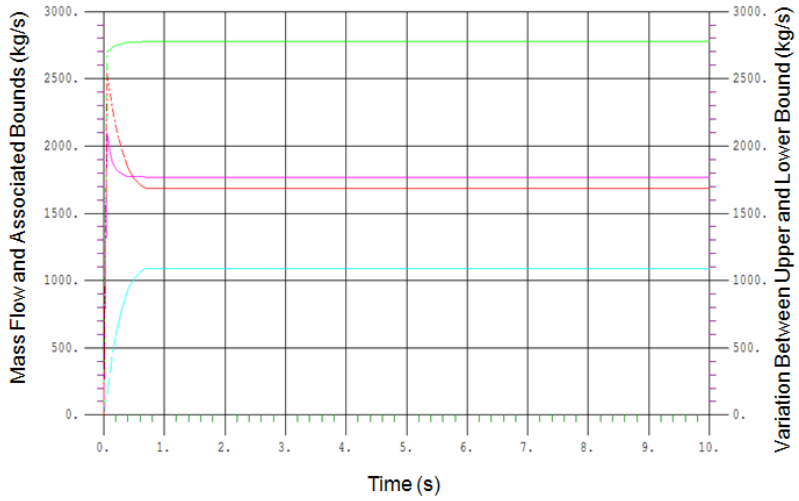

Figure 6 – Mass flow through the pipe with associated uncertainty limits

5. References

[1] www.relap.com.

[2] C. M Allison and J.K Hohorst, “Role of RELAP/SCDAPSIM in Nuclear Safety”, International Topical Meeting on Safety of Nuclear Installations, Dubrovnik, Croatia, September 2008.

[3] C. M. Allison, R. J. Wagner, L.J.Siefken, J.K. Hohorst, “The Development of RELAP5/SCDAPSIM/MOD4.0 for Reactor System Analysis and Simulation”, Proceedings of the 7th International Conference on Nuclear Option in Countries with Small and Medium Electricity Grids, Dubrovnik, Croatia, (May 2008).

[4] www.sdtp.org.

[5] C. M Allison and J.K Hohorst, “SDTP—Developing Technology for the Nuclear Industry”, 13th International Conference on Nuclear Engineering, ICONE13-50979, Beijing, China, May 16–20, 2005.

[6] RELAP5 Code Development Team, “RELAP5/MOD 3.3 Code Manual, Vol. 1-8”, NUREG/CR-5535/Rev1 (December, 2001).

[7] SCDAP/RELAP5 Development Team, “SCDAP/RELAP5/MOD3.2 Code Manual, Vol. 1-5”, NUREG/CR-6150, INEL-96/0422, (July, 1998).

[8] M. Perez, F. Reventos, R. J. Wagner, C. M. Allison, “Integrated Uncertainty Analysis using RELAP/SCDAPSIM/MOD4.0”, NUTHOS-7: The 7th International Topical Meeting on Nuclear Reactor Thermal Hydraulics, Operation and Safety, Seoul, Korea, October 5-9, 2008.

[9] M. Perez, F. Reventos, R. J. Wagner, C. M. Allison, “Integrated Uncertainty Analysis using RELAP/SCDAPSIM/MOD4.0”, The 13th International Topical Meeting on Nuclear Reactor Thermal Hydraulics (NURETH-13),Kanazawa City, Japan, September 27-October 2, 2009.

[10] Hou Dong, Meng Lin, R. J. Wagner, C. M. Allison, J. K. Hohorst, “Development of a 3D Reactor Kinetics Model for RELAP/SCDAPSIM/MOD4.0 for PWR Applications”, Paper submitted to NUTHOS-8, Shanghai, China, October 18-22, 2010.

[11] C. M. Allison, B. S. Allison, U. Luettringhaus, J. K. Hohorst, “Application of RELSIM-RELAP/SCDAPSIM for University Training and Simulator Development”, Proceedings of the 18th International Conference on Nuclear Engineering, ICONE18, Xi’an China, May 17-21, 2010.

[12] K. D. Kim, S. W. Lee, C. M. Allison, “Development of Visual System Analyzer Based on the Best-Estimate Code RELAP/SCDAPSIM”, Proceedings of ICONE-13, Beijing, China (May 2005).

[13] C. Chavez-Mercado, J. K. Hohorst, C. M. Allison, ”National Autonomous University Of Mexico RELAP/SCDAPSIM-Based Plant Simulation and Training Applications to the Laguna Verde NPP, Proceedings NUTHOS-6, Nara, Japan (October 2004).

[14] S. S. Wilks, “Determination of sample sizes for setting tolerance limits,” Annals of Mathematical Statistics, vol.12, no. 1, pp. 91-96, 1941.

[15] S. S. Wilks, “Statistical prediction with special reference to the problem of tolerance limits,” Annals of Mathematical Statistics, vol. 13, no. 4, pp. 400-409, 1942.

Development of a numerical tool for safety assessment and emergency management of experimental reactors

L. MAAS, A. BEUTER
Reactor Safety Division, Institut de Radioprotection et de Sûreté Nucléaire (IRSN)
31, Avenue de la Division Leclerc
92260 Fontenay-Aux-Roses - France

C. SEROPIAN
Major Accident Prevention Division, Institut de Radioprotection et de Sûreté Nucléaire (IRSN)
BP 3
13115 Saint-Paul-lez-Durance Cedex - France

ABSTRACT

The Institute of Radiological Protection and Nuclear Safety (IRSN) acts as technical support to French public authorities. Among its duties, one important item is to provide help for emergency situations management in case of an accident occurring in a French nuclear facility. In this framework, IRSN develops and applies numerical tools dealing with containment management issues. Up to now IRSN has not got any specific tool for experimental reactors. Accordingly, it has been then decided to extend the ASTEC code, devoted to severe accident scenarios for Pressurized Water Reactors, to this kind of reactors. This lumped-parameter code, co-developed by IRSN and GRS (Germany), covers the entire phenomenology from the initiating event up to fission products release outside the reactor containment, except for the steam explosion and the mechanical integrity of the containment. A first application to experimental reactors was carried out to assess the High Flux Reactor (HFR) operator's improvement proposal concerning the containment management during accidental situations. This reactor, located in Grenoble (France), is composed of a double wall containment with a pressurized containment annulus preventing any direct leakage into the environment. Until now, in case of severe accidents (mainly core melting in pool, explosive reactivity accident called BORAX), the HFR emergency management consisted in isolating the containment building in the early stage of the accident, to prevent any radioactive products release to the environment. The operator decided to improve this containment management during accidental situations by using an air filtering venting system able to maintain a slight sub-atmospheric pressure in the reactor building. The operator's demonstration of the efficiency of this new system is mainly based on containment pressure evaluations during accidental transients. IRSN assessed these calculations through ASTEC calculations. Finally, a global agreement was found with the operator's conclusions. Globally, it demonstrates that ASTEC is a convenient tool for safety assessment and emergency management of experimental reactors. Future work is planned to extend modeling to core and pool, as to enable simulating the complete accident and predict fission products releases.

1 Introduction

As technical support to French public authorities, one of the duties of the Institute of Radiological Protection and Nuclear Safety (IRSN) is to improve emergency situations management in case of an accident occurring in a French nuclear facility. In this framework, IRSN develops and applies numerical tools for dealing with containment management issues. Up until now, IRSN did not have a specific tool for experimental reactors. Accordingly, it has been then decided to extend the use of the ASTEC code [1], devoted to severe accident scenarios for Pressurized Water Reactors, to this kind of reactors. A first

application to experimental reactors was carried out to assess the High Flux Reactor (HFR) operator's improvement proposal concerning the containment management during accidental situations. The final purpose is to evaluate the radiological releases into the environment. As a first step, the pressure evolution in containment has been computed for three severe accidents scenarios: core melting under water, core melting in air and the explosive reactivity accident called BORAX. This paper describes the ASTEC modelling and presents some calculations results demonstrating the capabilities of the code to provide valuable support for safety analysis.

2 Overview of the ASTEC code

The ASTEC (Accident Source Term Evaluation Code) integral code is being co-developped by IRSN and GRS (Gesellschaft fur Anlagenund Reaktorsicherheit). It simulates the complete scenario of a severe accident in a Pressurized Water Reactor, from the initiating event up to fission products release outside the reactor containment. ASTEC consists of several modules dedicated to specific phenomena: for instance, CPA for the thermal-hydraulics and aerosol behaviour in containment, ISODOP for the fission products and actinide isotope decay, SOPHAEROS for the transport of fission products… They can be used in a coupled mode or a stand-alone mode. The validation of the code is based on a large number of separated-effects tests and integral experiments [3]. The applications are source term evaluation studies, Probabilistic Safety Assessment level 2 studies (PSA-2) and accident management studies for PWR.
As far as research reactors are concerned, some discrepancies exist with power plants, especially design, power level and operating mode. Nevertheless, the containment behaviour is driven by the same physical phenomena and that is why the code can be applied for studying situation management. The CPA module, devoted to thermohydraulics in containment, is based on a "lumped-parameter" approach (0D zones connected by junctions). Energy and mass equations are solved in each zone, and mass transfers between zones are described by momentum equations. CPA is able to take into account all the phenomena occurring in containment, especially evaporation, condensation, and heat transfers (forced and free convection, radiation, 1D conduction in structures).

3 HFR computations

3.1 HFR description and containment modelling

The HFR, located in Grenoble (France), operates with a thermal power of 57 MW and produces an intense source of neutrons entirely dedicated to fundamental research. The core consists of a single fuel element made of 280 plates highly enriched in uranium 235 (93%) with aluminium cladding. It is cooled and moderated by heavy water. The reactor containment building has two walls: an inner concrete wall and an outer metal shell (figure 1). The space between these two walls is pressurized at 135 mbar compared to the reactor building, which is under slight sub-atmospheric pressure (999 mbar). Until now, in case of severe accidents, the HFR emergency management consisted in isolating the containment building in the early stage of the accident, to prevent any radioactive products release to the environment. The operator decided to improve this containment management during accidental situations by using an air filtering venting system able to maintain a slight sub-atmospheric pressure in the reactor building.
The HFR containment was modelled using five compartments (figure 1). Two compartments have been used for the operation area to model the pool and the storage pool separately, but also to take into account possible convection movement. Internal structures made of concrete or steel, like the travelling crane, are taken into account. The leakage from the pressurized containment annulus to the containment building is given by experimental correlations established by the operator. The containment depressurization system is taken into account by imposing an outgoing mass flow rate.

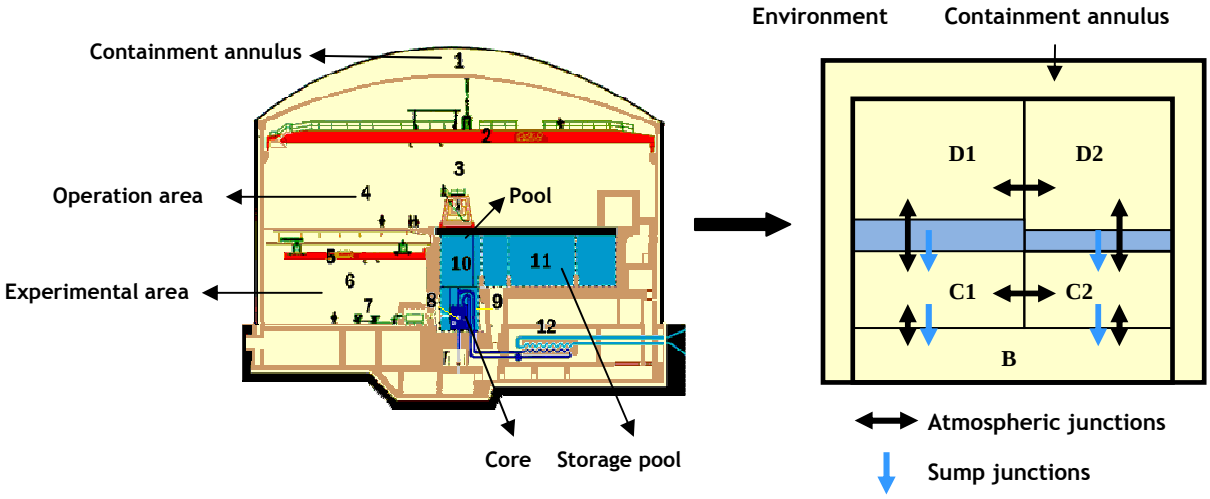

Figure 1: HFR cross section and ASTEC modelling

3.2 Accidental transient simulations

Three scenarios were studied with the CPA module of ASTEC: core melting under water, core melting in air and the explosive reactivity accident called BORAX. The two containment managements have been simulated: current static containment based on the building isolation and dynamic containment using an air filtering venting system proposed by the operator. Studying the current management and make comparisons with the operator calculations was a first step before assessing the efficiency of the new venting system.
For each transient, operating instructions concerning the containment management are taken into account: indeed, the containment annulus pressurization is reduced from 135 to 70 mbar in order to reduce the leakage mass flow rate from the containment annulus. This limits the containment inflation while also allowing sufficient overpressure in the annulus in the case of combustion of cold and hot sources.

3.2.1 Core melting under water

The first scenario is a conventional loss of coolant accident, occurring for example in case of a partial or total plugging of the fuel element channels by a moving object. The decay heat is released into the water.
In the case of containment isolation, a fast pressure increase is observed during the first stage of the accident, when the leakage from the pressurized containment annulus and the steam produced by the decay heat released into the pool are maximal (see the black curve on figure 2).
A good agreement was found with the operator calculations: the depressurization system is powerful enough to maintain the containment under sub-atmospheric pressure (see the blue curve on figure 2).

3.2.2 Core melting in air

The second scenario is a loss of coolant accident during the fuel handling. It can be the consequence of failures leading to the obstruction of the fuel element reflood. The decay heat is released into the air and the concrete. A good agreement was also found with the operator results (see figure 2).

The case of a core melting in air inside the reactor cavity has also been studied, even if such an accident is totally excluded. A sequence of events leading to the core top uncovering after 24 hours has been considered. The operator is planning on using this delay to depressurize the containment building from 999 to 980 mbar before the core melting in air. The calculations highlighted that this operating instruction is required to maintain a sub-

atmospheric pressure in the containment building during the two first hours of the accident while using the depressurization system (see figure 3).

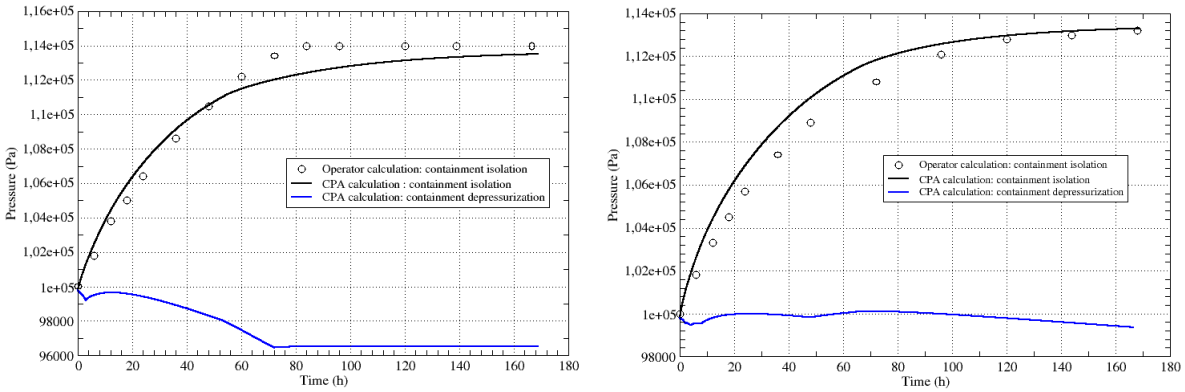

Figure 2: Containment pressure in case of core melting under water (on the left) and in case of core melting in air during the fuel handling (on the right)

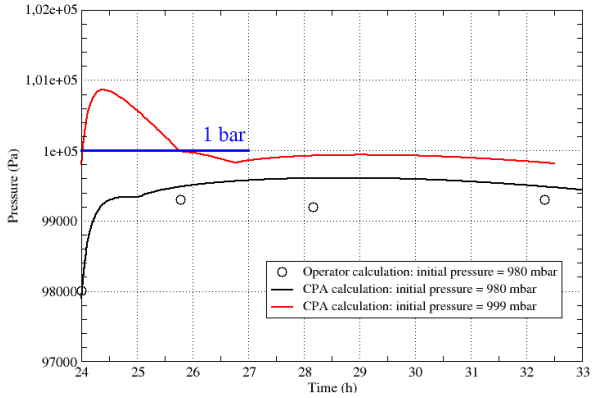

Figure 3: Containment pressure in case of core melting in air inside the reactor cavity while using the depressurization system

3.2.3 Explosive reactivity accident

The third scenario is a reactivity accident occurring in case of a fast control rod withdrawal. The reactivity injection can lead to the cladding melting and generate a steam explosion ejecting a large amount of water outside the pool. The pressure peak resulting from this massive injection of hot water in the operation area is difficult to evaluate. The quantity of steam produced depends on the water mass and the exchange with the air, increased by the spray fragmentation and velocity. This phenomenon was modeled using the spray module of ASTEC. It was possible to control the quantity of steam produced by simply tuning the droplets diameter. Owing to the explosive nature of this accident, the combustion of hot and cold sources was also taken into account by injecting an extra energy source.

A parametric study showed that the initial pressure peak is included within the range of 117 to 172 mbar, depending on the spray features (water mass and droplets diameter). A sub-atmospheric pressure is reached in the containment building after 2 to 4 hours with the depressurization system (see figure 4).

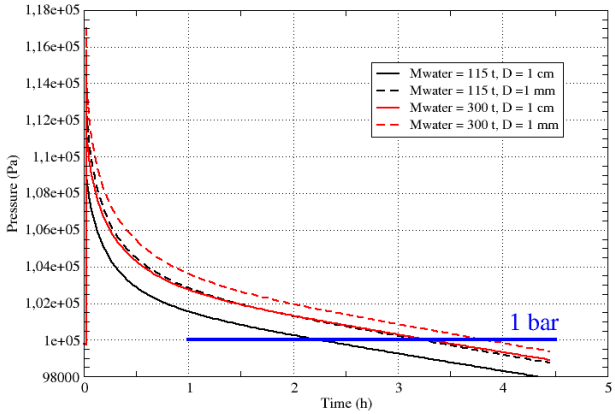

Figure 4: Containment pressure in case of the explosive reactivity accident called BORAX while using the depressurization system

4 Conclusion

First application of ASTEC to research reactor has been carried out without modification of the code. It deals with the RHF operator's improvement proposal concerning the containment management during accidental situations. Three severe accidents scenarios have been simulated: core melting in water, core melting in air and the explosive reactivity accident (BORAX). A global agreement was found with the operator's conclusions. Sensitivity to relevant parameters or hypothesis such as the operating instructions in case of accidental situations has been stressed by the calculations. The use of such a tool made the safety assessment more efficient. Besides, the input deck is now available to simulate the thermal-hydraulics behaviour of the containment for different accidental situations. All the information given by the code can be used for crisis management. Indeed, for each simulated accident, new tables can be prepared with results of pressure evolution in the reactor building, useful to know the ventilation mass flow rate and then evaluate the consequences on the environment.
The input deck can be extended to core and pool modeling in order to evaluate radiological consequences due to the release of FP's. Developments are also planned in ASTEC to simulate with a simplified modelling the growth of the bubble during a BORAX accident. Furthermore, it demonstrates that ASTEC is a convenient tool for safety assessment and emergency management of experimental reactors.

References

[1] J.P. Van Dorsselaere, C. Seropian, P. Chatelard, F. Jacq, J. Fleurot, P. Giordano, N. Reinke, B. Schwinges, H.J. ALLELEIN and W. Luther, "The Astec integral code for severe accident simulation", Nuclear Technology, vol. 165, march 2009

[2] I. Kljenak, M. Dapper, J. Dienstbier, L.E. Herranz, M.K. Koch and J. Fontanet, "Thermal-hydraulics and aerosol containment phenomena modelling in ASTEC severe accident computer code", Nuclear Engineering and design 240, 2010

[3] J. Vendel, J. Malet, A. Bentaib, H.J. Allelein, S. Schwarz, E. Studer, H. Paillère, K. Fischer, M. Houkema, "The 12th International Topical Meeting on Nuclear Reactor Thermal-Hydraulics (NURETH-12), Conclusions of the ISP-47 'Containment thermal-hydraulics"

MODELING IR-8 RESEARCH REACTOR OF RRC KI FOR PRECISION NEUTRONICS CALCULATIONS

D.S. OLEYNIK, V.A. NASONOV, N.I. ALEXEEV,
D.Y. ERAK, V.N. KOCHKIN
RUSSIAN RESEARCH CENTER «KURCHATOV INSTITUTE»
RRC KI, Kurchatov Sq 1., Moscow 123182, Russia

The IR-8 pool type research reactor of RRC KI was commissioned in 1981 for carrying out fundamental and applied researches in various areas of science and technique. MCU-PTR code with the MCUDB50 constants library was created to ensure the safe operation of the reactor and for the calculation support of experimental research. The MCU-PTR code is intended for simulation of neutron transport by means of the Monte Carlo method on the basis of evaluated nuclear data taking into account of changes in the nuclide composition of materials in interaction with neutrons.

Full-detailed 3D mathematical models of different states of the IR-8 reactor were created for precision neutronics calculations with use of MCU-PTR code. The code verification for pool and tank type research reactors performed based on IHECSBEP Criticality Benchmark Experiments and experiments carried out at the IR-8 reactor. The MCU-PTR code is currently used for calculations of the IR-8 reactor taking into account of fuel burn-up with HEU or LEU, poisoning of the beryllium reflector and burn-up absorber in CPS rods.

1. The IR-8 reactor description

The IR-8 reactor [1] is a pool type research reactor with power up to 8 MW, using water as moderator, coolant and top of biological shielding.
The reactor core consists of 16 IRT-3M type fuel assemblies (FA) with UO_2 fuel of 90% enrichment. The core and the reflector are installed in the vessel and rested on the support grid near the pool bottom. The pool depth is 11 m. All of the 13 CPS rods use boron carbide as an absorber.

The reactor has 12 horizontal experimental channels to extract neutron beam (beam tubes) for carrying out fundamental and applied researches in various areas of science and technique. The IR-8 reactor construction permits possibility installation many vertical experimental channels (VEC) for irradiation of fuel, of structural materials and isotopes production.
The main objective of the reactor is to provide a high thermal neutron flux density in the large beryllium reflector.
Now the reactor operates at power up to 6 MW. Main parameters of the IR-8 reactor are presented in Table 1 [2].

2. Программа MCU-PTR

MCU-PTR code [3] is developed for simulation of neutron and photon particles transport by analog and non-analog Monte Carlo methods. The simulation is realized on the basis of the evaluated nuclear data considering depletion process.

The data bank of the code is MDBPTR50. All necessary characteristics of nuclides being set as burnable in initial data are located in BURN part of the data bank. That contains approximately 1100 nuclides.

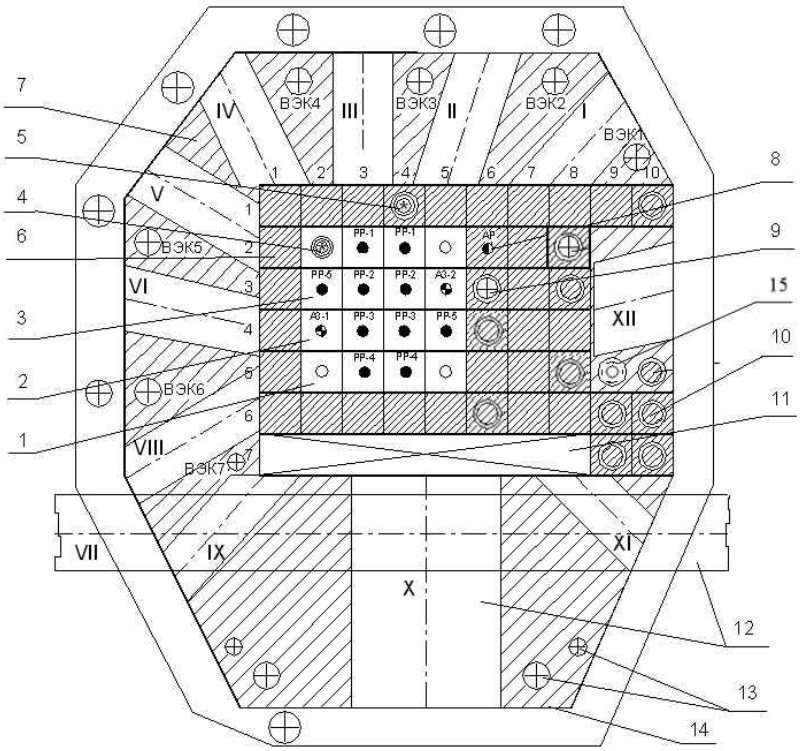

1 - IRT-3M six-tube FA;
2 - IRT-3M six-tube FA with safety rod; **3** - IRT-3M six-tube FA with shim-safety rod; **4** - IRT-3M four-tube FA with an ampoule rig (AR);
5 - beryllium block with an ampoule rig; **6** - beryllium block 69×69 mm; **7** - block of stationary beryllium reflector;
8 - beryllium block with automatic regulating rod;
9 – beryllium block with experimental channel;
10 - beryllium blocks with plugs; **11** - lead shield;
12 - beam tubes; **13** – holes for experimental channels;
14 – reactor vessel;
15 – experimental channels.

Fig 1. Cross section of the IR-8 core and of the reflector

Power, MW	6,0
Number of FAs in the core	16
Core volume, l	47,4
Mass of ^{235}U in the core with “fresh” FAs, kg	4,35
Maximum reactivity margin of the core in the partial reloading regime , %Δk/k	12,0
Total reactivity worth of CPS rods, %Δk/k:	
- safety rods	4,6
- shim-safety rods and automatic regulating rod	26,3
Maximum neutron flux with ampoule rigs in the reflector *), $cm^{-2}\cdot s^{-1}$:	
• thermal:	
- in 6-3 cell	$4,9\cdot10^{13}$
- at the face of a horizontal channel	$9,9\cdot10^{13}$
- in a VEC	$4,8\cdot10^{13}$
• fast (E>0,5 MeV):	
- in 6-3 cell	$3,3\cdot10^{13}$
- in VEC	$1,3\cdot10^{12}$
- in AR (6-4 cell)	$2,3\cdot10^{13}$
- in AR (7-3 cell)	$7,7\cdot10^{12}$
- in AR (8-3 cell)	$2,9\cdot10^{12}$

*) Calculation by MCU-PTR code

Tab 1: Main parameters of the IR-8 reactor with ARs in the reflector

3. Modeling of the IR-8 Reactor

For full-scale simulation of the IR-8 reactor were originally modeled and tested in calculations of the cells with IRT-3M FAs. Calculating geometrical models of FA (fig. 2) within the reactor core are completely identical to sizes of IRT-3M FA. Zones of top and bottom ends of the FAs and beryllium reflector are presented in homogeneous approach. The set of full - scale 3-D geometrical models for various variants of IR-8 reactor loadings is created. Cross- and longitudinal- sections of one of the IR-8 reactor calculating models are presented on fig. 3, 4 and 5.

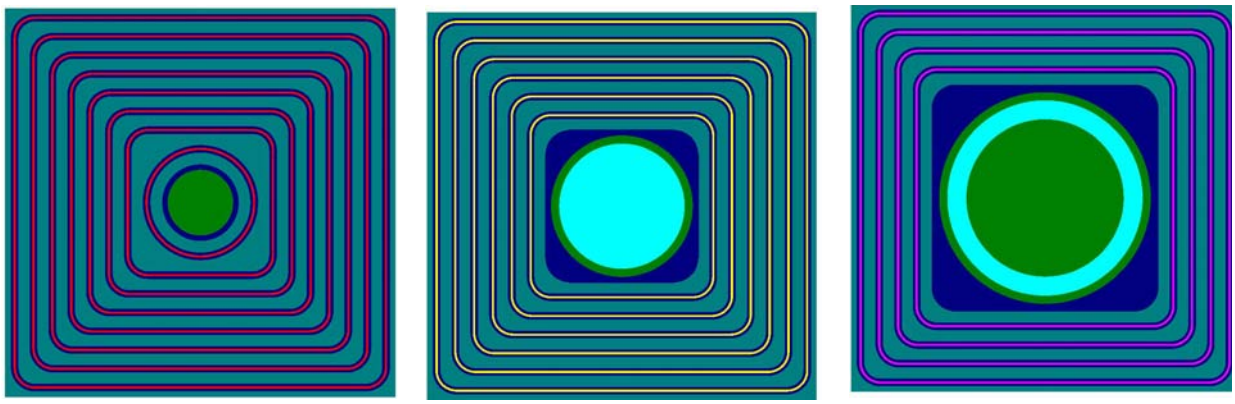

Fig. 2 Cross-sections of IRT-3M FA's calculating geometry

Numerical 3-D heterogeneous model of the IR-8 reactor in MCU-PTR code is presented as registration zones which structure is described by values of nuclear concentrations of the nuclides.
The main objective of the reactor is to provide a high thermal neutron flux density in the large beryllium reflector. So the reactor model contains 30 layers of fuel height; in a layer each meat of fuel element has its own registration zone. All fuel is in 2880 registration zones. CPS rod's absorber is divided into 900 zones (30x30). So total number of registration zones in the model is approximately 20000.
Variants of input files represent modeling of different IR-8 reactor operation stages for calculating its various conditions taking into account of fuel burn-up, poisoning of the beryllium reflector and burn-up absorber in CPS rods. The full - scale numerical 3-D model of the IR-8 reactor in MCU-PTR code has about 100000 lines [3].

4. Some results

Verification has been implemented on the basis of benchmarks which are stated in IHECSBEP and IR-8 experiments. Deviation of calculated effective multiplication factor from results of benchmarks with low-enriched uranium fuel (below 6,5%) [4, v. 4, LCT-053, LCT-061, LCT-070, LCT-075, LCT-085, LCT-094] is presented on Fig. 6. There are errors of our result are shown on the figure also. They are being included experimental error (0,3%) and statistical uncertainty of the calculation (0,2%).
23 bechmarks [4, v. 2, HCT-003, HCT-006, HCT-007, HCT-008] have been calculated to prove evaluated nuclear data for high-enriched uranium fuel (80%) (Fig. 7). There are good coincidence between MCU-PTR code and MCNP-4a results. Standard deviation of the results by MCU-PTR code from experimental data is approximately equal to 0,5 %. Mean values of k_{eff} over 23 benchmarks are equal to 1,0008±0,0048, 1,0026±0,0072 and 1,0000±0,0044 for MCU-PTR, MCNP-4a and experimental investigations accordingly. There are errors of our result are shown on Fig. 7 also. They are being included experimental error (0,44%) and statistical uncertainty of the calculation (0,2%).
There were studied and numerically reconstructed history of the IR-8 reactor since 1981 taking into account of fuel burn-up in the core, of ^{10}B burn-up in the CPS rods and the

poisoning of the beryllium reflector of the transmutation products.

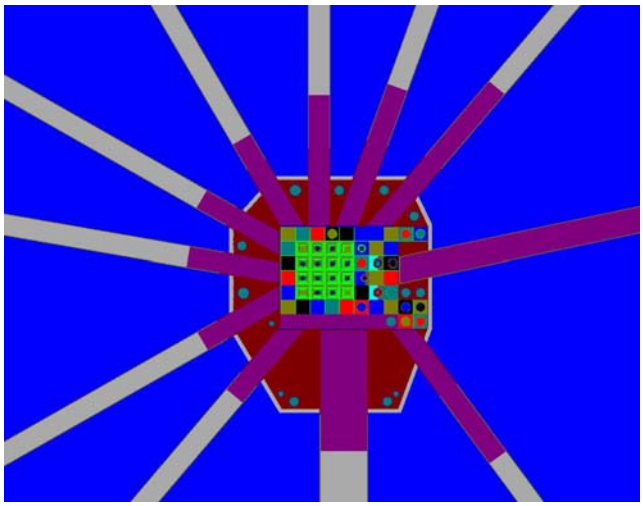

Fig. 3. Cross-sections of the IR-8 reactor calculating models with the beam tubes

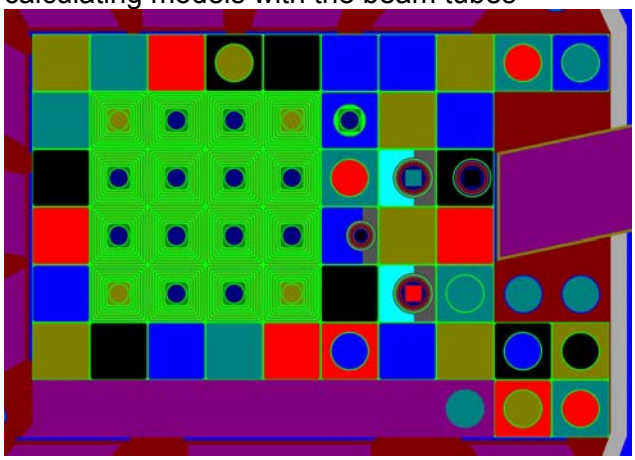

Fig. 4. Cross-sections of the IR-8 reactor core and of the removable beryllium blocks calculating models

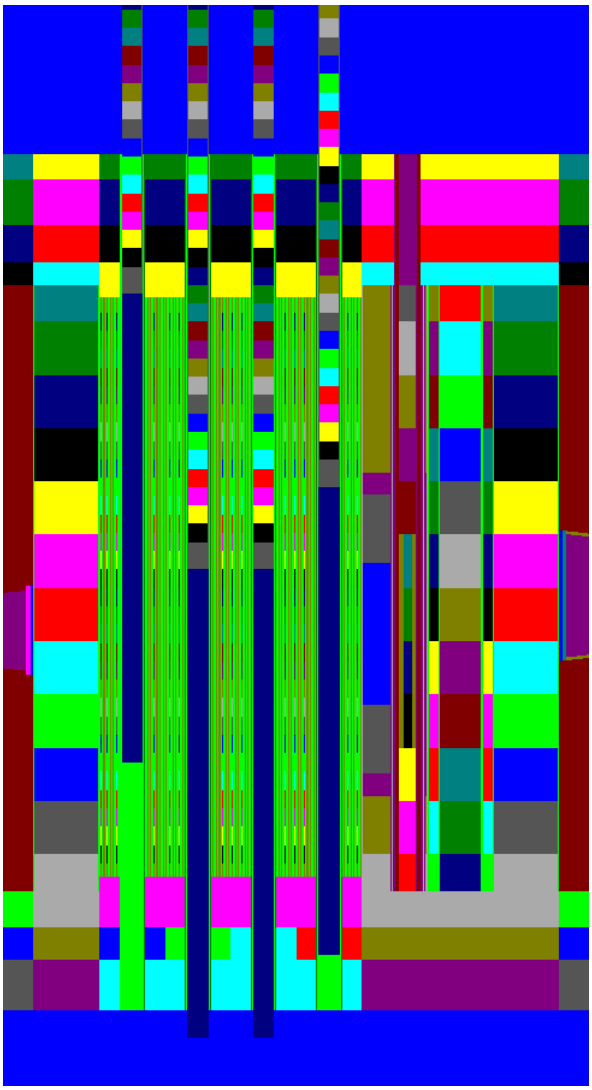

Fig. 5. longitudinal-sections of the IR-8 reactor calculating models with ARs in the reflector

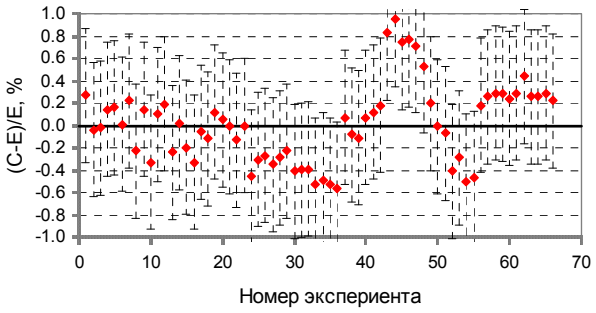

Fig. 6. Deviation of the calculated values of k_{eff} from the data in benchmark experiments with LEU

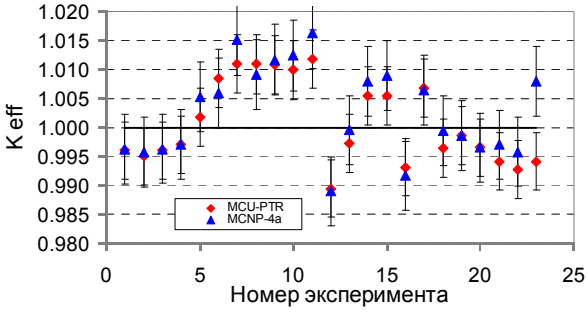

Fig. 7. Results of calculations of the critical experiments with HEU

The IR-8 reactor was operated for 77 cycles until 2010. The calculated results of critical states of loadings in the beginning of cycle with Xe-free core and core with equilibrium concentrations of Xe are presented in Table 2.

# loading	# cycle	The IR-8 reactor core	
		Xe-free	Xe
2008-09	69	1.0035	1.0077
2008-09a	70	1.0060	1.0077
2008-11	71	1.0043	1.0077
2009-01	72	1.0041	1.0017
2009-03	73	1.0023	1.0026
2009-04	74	1.0024	1.0005
2009-05	76	1.0060	0.9980
The average value of k_{eff}		1,0041	1,0037

Tab 2: The calculated results of k_{eff}

The calculated and experimental results of the fast neutron fluxes with E> 0.5 MeV in the cells of the IR-8 reflector are presented in Table 3. As the neutron-activation detectors used metal foils: ^{54}Fe [^{54}Fe(n,p) ^{54}Mn] and ^{93}Nb [^{93}Nb(n,n') ^{93m}Nb]. The calculated results are within experimental errors.

Cell	Experimental channel with	$\Phi_{E>0.5}\times10^{-12}$, $s^{-2}\cdot c^{-1}\cdot MW^{-1}$	
		Calculation	Experiment (Fe / Nb)
6-4	Air	3,87	3,94±0,43/3,85±0,41
	AR-1	3,89	4,29±0,51
7-3	Air	1,31	1,34±0,14/1,21±0,13
	AR-2	1,27	1,24±0,13
8-3	Air	0,46	0,436±0,052/0,423±0,049
	AR mock-up	0,35	0,432±0,045/0,382±0,040

Tab 3: The fast neutron fluxes in the cells of the reflector

5. Conclusion

The MCU-PTR code with MDBPTR50 evaluated nuclear data bank MDBPTR50 is developed to provide Monte-Carlo simulation of neutron and photon transfer accounting depletion.
The code hasn't verificated completely for calculation of pool and tank types research reactors with HEU and LEU yet, but critical experiments from international data bank IHECSBEP and on experiments, performed in RNC KI were calculated.
For that purpose the detail full-scale 3D mathematical model of various states of IR-8 reactor has been developed.
MCU-PTR code is used as calculation support for IR-8 and to provide fundamental and applied investigations of the reactor.

References

[1] Ryazantsev E.P., Nasonov V.A., Egorenkov P.M. et al. Contemporary status and employment perspectives of the IR-8 reactor. International scientific conference «RESEARCH REACTORS IN XXI CENTURE».MOSCOW, June 20-22, 2006.
[2] Erak D.Y., Nasonov V.A., Taliev A.V et al. Main parameters of the IR-8 reactor with ampoule rigs in the reflector. Pre-print IAE-6613/4, M., 2009.
[3] Nasonov V.A., Alexeyev N.I., Erak D.Y. et al. Development of the calculation-experimental methods of determining the parameters of neutron flux distribution in the IR-8 reactor of RRC KI for fundamental and applied researches. Pre-print IAE-6579/4, M., 2009.
[4] International Handbook of Evaluation Criticality Safety Benchmark Experiments, NEA/NSC/DOC(95)03, September 2008 Edition. (vol.1-vol.6)
[5] International Handbook of Evaluation Reactor Physics Benchmark Experiments, NEA/NSC/DOC(2006)1, March 2009 Edition.

COUPLED 3D NEUTRONIC AND THERMOHYDRAULIC CALCULATIONS FOR A COMPACT FUEL ELEMENT WITH DISPERSE UMo FUEL AT FRM II

H. BREITKREUTZ, A. RÖHRMOSER, W. PETRY
Forschungsneutronenquelle Heinz Maier-Leibnitz (FRM II), Technische Universität München
85747 Garching – Germany

ABSTRACT

The newly developed X² program system is intended to be used for high-detail 3D calculations on compact research reactor cores. Using this system, the efforts to calculate scenarios for a new fuel element for FRM II using disperse UMo (8wt% Mo, 50% enrichment) are continued. By now, a radial symmetric core model with averaged built-in components for the D_2O tank is used.

Two different scenarios are compared: The minimum fuel density of 7.5 g U/cm³ and 8.0 g U/cm³ with 60 days cycle length. In addition, two "flux loss compensating" scenarios based on 8.0 g U/cm³ with 10% higher power / longer reactor cycles are regarded.

1. Introduction

1.1 FRM II, Disperse UMo

The core of FRM II consists of only one single fuel element, a compact core with 113 evolute shaped fuel plates. Currently, a disperse U_3Si_2-Al fuel with densities up to 3.0 g U/cm³ is employed. The degree of enrichment is 93% (HEU). In terms of the RERTR program, cores with a higher uranium density and consequently lower enrichment are studied. For this, disperse UMo-Al (8 wt% Mo) is a promising candidate. For the particular geometry of the FRM II compact core, this would allow a decrease of the enrichment down to 50% (MEU).

FRM II performed general feasibility calculations for a compact core of this type [13] and is also engaged on the experimental side of the development of the new fuel [3].

The general conditions for the fuel conversion of FRM II are:

- In all aspects the new core has to be as save as the current one
- The achievable cycle length must be at least 60 days at 20 MW power (today's value)
- The neutron flux and quality have to be as high as currently (only marginal losses)
- Any conversion to lower enrichment has to be economically reasonable, i.e. operation costs increase only marginally

In the framework of this paper, it will be discussed how some of these requirements can be met using disperse UMo. The approaches are straight-forward, all design parameters are inherited directly from the current fuel element. In addition, two hypothetical scenarios to compensate the flux loss by a higher reactor power or a longer cycle length are given.

1.2 The X² program system

The X² program system is a new, coupled calculation system developed at FRM II. It couples the Monte Carlo code MCNPX (currently version 2.7.B) [1], the CFD code CFX (ANSYS, version 12) [2] and the burn-up program MonteBurns [4]. It is specialised on the simulation of compact research reactor cores.

The code system was validated by a code-to-code comparison on the results of the current fuel element of FRM II as calculated by [7,8,9] as well as comparisons to measured data as far as available [10]. All calculations are conducted in 3D as far as possible. Oxide layers, burn-up and heat distributions can be considered. The principal program flow of X² is shown in fig. 1. More details on the implementation in X², the choice of codes and the application to FRM II can be found in [11,12].

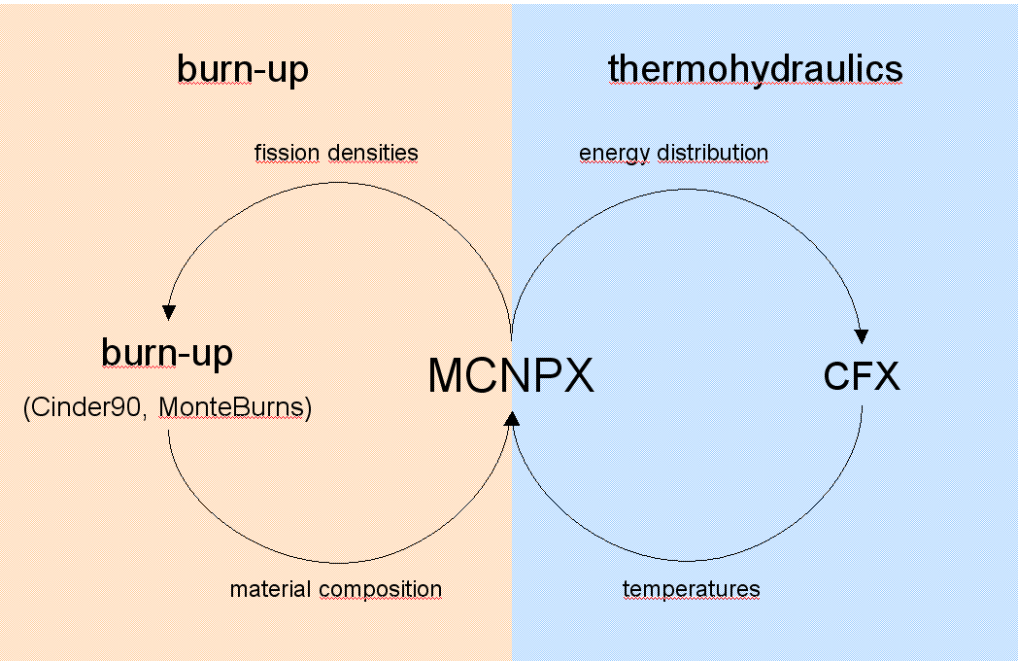

Fig 1: X² program flow

2. Scenarios

As mentioned before, two different main conversion options are considered. The minimum uranium density at 50% enrichment to guarantee a reactor cycle length of 60 days with disperse UMo is 7.5 g U/cm³. A higher density of 8.0 g U/cm³ permits further installations in the reactor or compensation for reactor degradation. It is obvious that a higher uranium density will worsen the neutronic and thermohydraulic properties of the core. Therefore, two “loss compensating” scenarios with a higher total power (22 MW instead of 20 MW) or a longer cycle length (66 d / 60 d) are discussed.

Figure 2 shows the predicted control rod driveway of FRM II for ulterior unchanged conditions compared to the current situation. The technical limit is a control rod position of +41 cm. The steeper slope at the very begin of the cycle (BOL) compared to the current situation originates from the lower excess reactivity due to the increased parasitic absorption from ^{238}U in the fuel. For the case of 8 g U/cm³ at 20

MW, the slope generally rises slower due to the higher remaining ^{235}U density during the cycle. The general steepening towards EOL is explained by the lower control rod reactivity worth as the rod position approaches it upper limit.

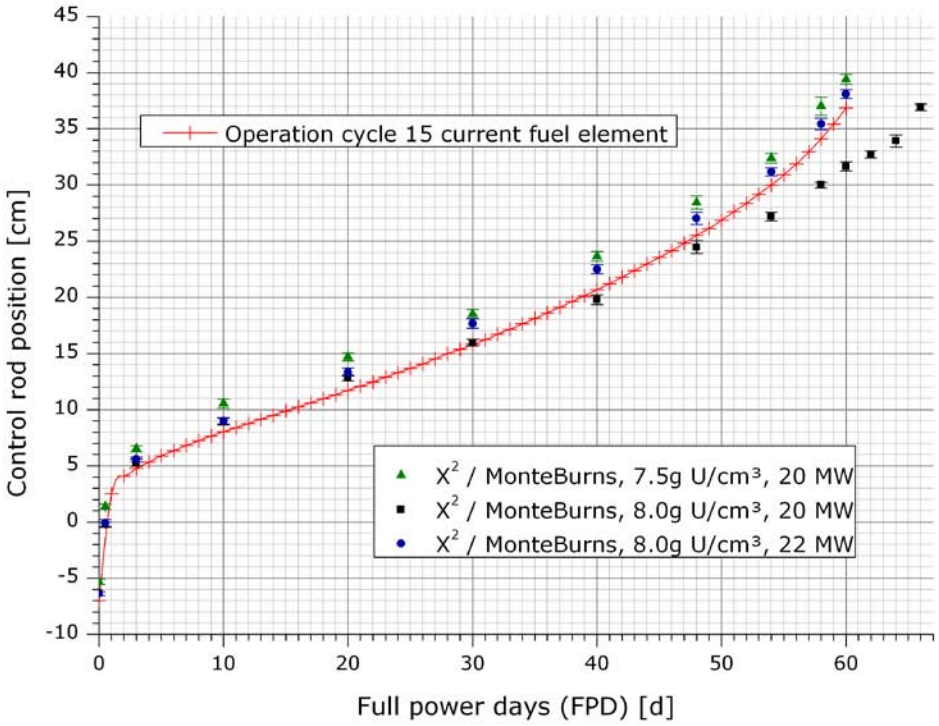

Fig 2: Predicted control rod driveway for different scenarios

An overview of the results of all four conversion scenarios and a comparison to the current situation can be found in table 1.

2.1 7.5 g U/cm³

Earlier calculations [13] already identified 7.7 g U/cm³ as the density to reach the same $\Delta\rho$ after 52 days of operation. Now, in a series of calculations, 7.5 g U/cm³ were identified as the minimum uranium density of disperse UMo to achieve a cycle length of 60 days. Despite the fact that the use of this minimum density leaves no room for optimisation of the reactor usage or compensation of the flux loss and reactor degradation, it has the less disadvantageous neutronic and thermohydraulic properties:

The maximum heat flux density rises to 401 W/cm² (up 5% from calculation for current situation), the maximum power density in the active zone rises by 7%. The maximum wall temperature rises only slightly by 1.5 K. The main drawback is a drop of the maximum neutron flux by 6.7%, as well as a drop of 6.2% of the cycle neutron yield in the BOL thermal flux maximum, $CNY(\vec{r}) = \int_0^T \phi(\vec{r},t) \cdot dt$.

However, experience with the current fuel element has shown that it is not only beneficial but necessary to have some reactivity reserve at the end of the cycle, which would not be the case with 7.5 U g/cm³.

2.2 8.0 g U/cm³

FRM II has always regarded 8.0 g/cm³ U-density as the most realistic solution for 50% enriched disperse UMo [13]. Therefore this scenario was analysed in greater detail and two options to compensate the resulting flux loss were studied. It is obvious that the flexibility gained by a higher uranium density has to be paid-off by less fortunate thermohydraulic and neutronic properties, amongst others a higher flux loss.

2.2.1 20 MW / 60 d

20 MW power and 60 days cycle length is the current situation at FRM II and the targeted minimum after the conversion of FRM II.

In the case of 8 g/cm³ uranium, the maximum heat flux density rises 6.5% to 407 W/cm². Wall and fuel temperatures are slightly higher than in the 7.5 g U/cm³-case but comparable. The maximum flux drops even more, -7.7%, as well as –7.1% for the cycle neutron yield in the flux maximum. The higher fuel density causes considerably higher local burn-up, $2.13 \cdot 10^{21}$ fissions/cm^3. This is 7.6% higher than in the current situation and 4.4% higher than in the 7.5 g U/cm³-case.

2.2.2 20 MW / 66 d

Increasing the cycle length is one option to compensate the flux loss caused by the higher uranium densities. However, an increase in the cycle length is limited by the maximum burn-up the fuel can handle.

Obviously, thermohydraulic properties remain unchanged from the 60 days case. The 10% extra cycle length overcompensates the loss in the cycle neutron yield by about 2%. However, a 8% higher local burn-up than with 60 days cycle length has to be handled, now $2.30 \cdot 10^{21}$ fissions/cm^3 in the maximum. Considering the present developments, it is rather unlikely that the fuel can withstand such a high a burn-up.

2.2.3 22 MW / 60 d

The third option, an increased reactor power while the cycle length is kept at 60 days, is of course the most welcome option but poses by far the highest burdens. As before, the very high burn-up has to be handled, but in addition higher demands on the cooling system have to be satisfied. The power increase would also require additional time- and labour-intensive licensing procedures for the reactor.

The power increase can be observed directly in all important thermohydraulic parameters: The maximum heat flux density at the plate surface has risen to

449 W/cm², 17.4% more than now. Compared to today's situation, the increase of the fuel temperature is 11.7 K, the maximum wall temperature rises by 7.1 K to 96.7°. According to 10% more power, the water heats up by 17.5 K instead of 15.9 K. The burn-up after 60 days is comparable to that after 66 days at 20 MW, $2.34 \cdot 10^{21}$ fissions/cm^3 (matching within estimated statistical uncertainty). In this scenario, the loss in CNY_{max} is overcompensated by about 2.5%. From the point of view of the users of FRM II, the situation remains unchanged from today if this scenario can be realised, which is very unlikely due to the implications discussed above.

2.3 Compact comparison

Quantity	Current	7.5g	8g	8g/66d	8g/22MW
Neutronic properties					
Max. burnup EOL [fis./cm^{-3}]	$1.98 \cdot 10^{21}$	$2.04 \cdot 10^{21}$	$2.13 \cdot 10^{21}$	$2.30 \cdot 10^{21}$	$2.34 \cdot 10^{21}$
Max. thermal flux [cm^{-2} s^{-1}]	$6.40 \cdot 10^{14}$	$5.97 \cdot 10^{14}$	$5.91 \cdot 10^{14}$	$5.91 \cdot 10^{14}$	$6.48 \cdot 10^{14}$
Cycle neutron yield [cm^{-2}]	$3.25 \cdot 10^{21}$	$3.05 \cdot 10^{21}$	$3.02 \cdot 10^{21}$	$3.31 \cdot 10^{21}$	$3.33 \cdot 10^{21}$
CNY_{max} compared to current		-6.2%	-7.1%	+1.8%	+2.5%
Thermohydraulic properties					
T_{max} fuel [°C]	102.9	108.2	108.2	108.2	114.6
T_{max} wall [°C]	89.6	91.1	91.8	91.8	96.7
T_{avg} outlet [°C]	52.9	52.9	52.9	52.9	54.5
q_{max} wall [W cm^{-2}]	382	401	407	407	449

Tab 1: Comparison of calculated neutronic and thermohydraulic properties (at BOL if not quoted otherwise)

The numbers quoted in tab. 1 apply to begin of live (BOL). The reactor model is axial symmetric and includes burn-up of the control rod. Temperatures were calculated by using UMo material data from Lee et al. [5], ranging from about 75 W/m K for 8g U/cc at room temperature to about 170 W/m K for 3.75g U/cc at 100°C. Due to lack of knowledge, no change of the thermodynamic properties of the fuel due to burn-up was included. A constant coolant inlet temperature of 37°C was assumed. Burn-up zones were chosen according to Röhrmoser et al. [6]. No oxide layer was taken into account as the data is for BOL.

3. Conclusions

It is apparent that 8g U/cc-22MW-60d is the most desirable scenario from the point of view of the scientists using the neutron source as it actually implies no change for users and instrument operators, but it is also the most demanding with respect to fuel qualification and reactor operation and very unlikely to be feasible. A scenario with 8g U/cc-20MW-60d produces the same cycle-neutron-yield without posing the burdens connected to an increase of the reactor power but still suffers from the very high burn-up of the fuel which is probably not achievable. However, if the current standard of 4 cycles per year should be kept, the shorter reactor down-times (-20%) will imply high demands on the operational team of the reactor. Accordingly, if feasible at all, only a fractional compensation of the flux loss due to the conversion seems to be a realistic option.

The two straightforward scenarios, a conversion without increase in cycle length and reactor power, deliver the most disadvantageous performance. Of those two, 8g

U/cc-20MW-60d is the most likely scenario, although it even underperforms 7.5g U/cc-20MW-60d. The latter leaves no room for increased reactor usage, neither does it contain any reactivity reserves to compensate reactor degradation due to aging or other flux depressing effects. Therefore, for a future-proof operation of FRM II using 50% enriched disperse UMo, a minimum uranium density of 8 g U/cm³ is required.

Acknowledgements

This work was supported by a combined grant (FRM0911) from the Bundesministerium für Bildung und Forschung (BMBF) and the Bayerisches Staatsministerium für Wissenschaft, Forschung und Kunst (StMWFK).

References

[1] D. B. Pelowitz et al. : MCNPX 2.7.B Extensions, LA-UR-09-04150, Tech. rep., Los Alamos National Laboratory (2009).
[2] ANSYS CFX Reference Guide (Release 12.0) (2009).
[3] Winfried Petry, Anton Röhrmoser, P. Boulcourt: UMo full size plates irradiation experiment IRIS-TUM – a progress report, Transactions of the RRFM 2008, Hamburg, Germany, 3/2008
[4] T. Poston, D.L.: User's Manual, Version 2.0 for MONTEBURNS Version 1.0, LA-UR-99-4999 (9 1999).
[5] S.H. Lee, C.K. Kim, J.M. Park: Thermophysical Properties of U-Mo/Al Alloy Dispersion Fuel Meats, International Journal of Thermophysics 28, p. 1578-1594, 10/2007
[6] Anton Röhrmoser, Winfried Petry: Swelling at the Fuel Edges of Irradiated Research Reactor Plates and Derivation of a Minimum Fuel Burnup Area for Qualification, RRFM 2010, Marrakech (to be published).
[7] A. Röhrmoser: Untersuchungen zur Kühlbarkeit eines neuartigen Kompaktkerns für Forschungsreaktoren, Master's thesis, Technische Universität München (1984).
[8] C. Döderlein: Untersuchungen zur Kühlbarkeit eines kompakten Reaktorkerns mit evolventenförmigen Brennstoffplatten, Master's thesis, Technische Universität München (1989).
[9] A. Röhrmoser: Neutronenphysikalische Optimierung und Auslegung eines Forschungsreaktors mittlerer Leistung mit Zielrichtung auf einen hohen Fluss für Strahlrohrexperimente, Ph.D. thesis, Technische Universität München (1991).
[10] Siemens Arbeitsbericht zur Thermohydraulischen Kernauslegung des FRM II (1996).
[11] Harald Breitkreutz, Anton Röhrmoser, Winfried Petry: 3-Dimensional Coupled Neutronic and Thermohydraulic Calculations for a Compact Core Combining MCNPX and CFX, Proceedings of ANIMMA 2009, Marseille
[12] Harald Breitkreutz, Anton Röhrmoser, Winfried Petry, X²: A coupled neutronic - thermohydraulic code system for compact research reactor cores, Physor 2010, Pittsburgh (to be published)
[13] Anton Röhrmoser, Klaus Böning, Winfried Petry: Reduced enrichment program for FRM II, Status 2004/05, Proceeding 9th International Meeting on Reduced Enrichment for Research and Test Reactors (RERTR), 2005

NEUTRONIC DESIGN OF SMALL REACTORS

L. CHABERT, T. BONACCORSI, M. BOYARD,
E. LEFEVRE, L. LAMOINE AND J. PIELA
AREVA-TA, CS 50497
F-13593 Aix en Provence CEDEX 3, France

ABSTRACT

Small reactors design is one of the main activities of AREVA TA. At the time, AREVA TA main projects are oriented towards research reactors and reactors for military naval propulsion. Due to differences in the physics and performances to meet, each kind of small reactor leads to specific modelling needs.
Many computing tools have been developed in order to successfully carry out these projects. These schemes are mainly based on the use of TRIPOLI, MCNP, APOLLO2 and CRONOS2 codes. In that framework, a multi-purpose pre/post processing tool named CHARM is being developed by AREVA NP in partnership with AREVA TA in order to integrate small reactors specification. CHARM is used to elaborate APOLLO2 input data while various dedicated tools are used to automatically generate TRIPOLI and MNCP input data. These 3D numerical models need a very accurate spatial description to perform specific calculations. As an example, for the JHR design, after calculating 3D burn up by APOLLO2/MOC models, the data is fed back into a TRIPOLI model used for safety analyses.
This paper presents our methodology for the small core design and 3 examples:

- The calculation scheme for the JHR (Jules Horowitz Reactor) neutronic studies. These design studies are a recent illustration of combined use of both deterministic and probabilistic codes,
- The use of CHARM, with the modelling of a JHR core. The purpose of CHARM-V2, based on Open Cascade Technology, is to provide a pre/post processing tool for APOLLO2/MOC, TRIPOLI4 and MCNP solvers,
- The depletion Monte Carlo calculation of a MTR core.

1. Introduction

AREVA TA (ex-TECHNICATOME) has a great experience in small-size reactors based on enriched uranium cores, moderated with light or heavy water: for instance, materials and test reactors along with propulsion reactors (both military and civil).
Historically, AREVA TA was created in 1972 following the merging of two CEA units (Commissariat à l'Energie Atomique), one specialized in material and test reactors and the other in propulsion reactors for the French Navy.

In these areas, our main projects are:

- Material and test reactors: …, ORPHEE, OSIRIS, PAT, CAP, RNG, RES, RJH-JHR (these two are still in progress),
- Propulsion reactors: "Le Redoutable", "Le Triomphant", "Rubis" and "Barracuda" class submarines, Charles de Gaulle aircraft carrier.

Our activity is also dealing with other nuclear reactor projects.

It is noticeable that we have been and remain the operator of many nuclear facilities:

- Test reactors, now all shutdown: PAT, CAP , RNG
- 1 test reactor under construction, nearing completion: RES
- Critical mock-up: AZUR

This point is a very important fact for the core and reactor design capability (direct feedback of reactor operation).

To achieve the high performances required, design of these reactors needs concerted action between many engineers in different technological and physical fields: mechanics, fuel and materials behaviours, command-control, instrumentation, thermal hydraulics, neutronics… All these technical fields are the basis of our activity.

Performances required for a material test reactor (MTR) are significantly different from these dedicated to a naval propulsion reactor (NPR), though many characteristics are common:
- The small size of the object that implies an appropriate treatment of the core-reflector interface and neutron leakage,
- High level of both security and availability requirement,
- Need of a high flexibility level in terms of experimental devices accommodation ability for MTR's and in terms of fast and frequent power transients for NPR's,
- The use of uranium fuel up to 20% U235 enrichment (LEU),
- The fluctuations required for the operating time of the core,
- Small series manufacturing.

To summarize, in comparison with power reactors like EPR, these small cores:
- Are more neutronically coupled (lesser needs for an online in-core survey),
- Needs higher uranium enrichments combined with a wide variety of burnable absorbers,
- Have more core-reflector interface effects,
- Require higher flexibility when in operation.

The purpose of this paper is to introduce the way we use neutronic codes for core design activities, in a strategy using both deterministic and stochastic codes.

2. Calculation schemes and codes

Due to differences in required performances, each type of small reactor leads to specific modelling needs. The following method is used to carry out our projects:
- Analysis of key values: fluxes, range of power, energy (life length), flexibilities, …
- Choice of the most reliable computing schemes and/or development (calculation codes, cross section libraries).

In terms of implementation, this method leads:
- To rely on both deterministic codes (APOLLO, CRONOS) and probabilistic codes (TRIPOLI [NPR, MTR], MCNP [MTR]) with associated advantages meaning respectively sturdiness on burn up calculations on the first hand and refinement in geometric description and better flexibility for what concerns calculated quantities (neutron and gamma heating, flux perturbation in experimental devices, ...) on the other hand,
- To use probabilistic codes at step 0 or in probabilistic depletion calculations using deterministic codes input (codes getting material balance from deterministic calculation objects) or in depletion calculations with ORIGEN and MONTEBURNS,
- To use machine human interface (MHI) allowing to generate the main part of datasets for the different codes from a single description of geometries and materials and also to analyze the results.

To illustrate these various issues, we give below three examples:
- The calculation scheme for the JHR (Jules Horowitz Reactor) neutronic studies,
- The use of the CHARM MHI, with the modelling of a JHR core,
- The depletion Monte Carlo calculation of a MTR core.

3. First example: Jules Horowitz Reactor – calculation scheme

The JHR core design studies [1] are a recent illustration of combined use of both deterministic and probabilistic codes and of implication of CEA teams in the MTR design projects.

In the beginning of the project, the CEA established the JHR-dedicated 3D regular geometry core calculation scheme HORUS3D/N V1 [1][6] based on the APOLLO2[4] and CRONOS2[3] codes.

This calculation scheme was an opportunity for us to study various shapes of regular cores. Taking this into account, we were then convinced to be able to find a control rod management and a refuelling strategy that would bound the 3D power factor, whatever the shape is. Step 0 Monte Carlo calculations allowed us to quickly find an optimum core shape which is an irregular geometry (close to a regular one) required by the high level of flux performances.

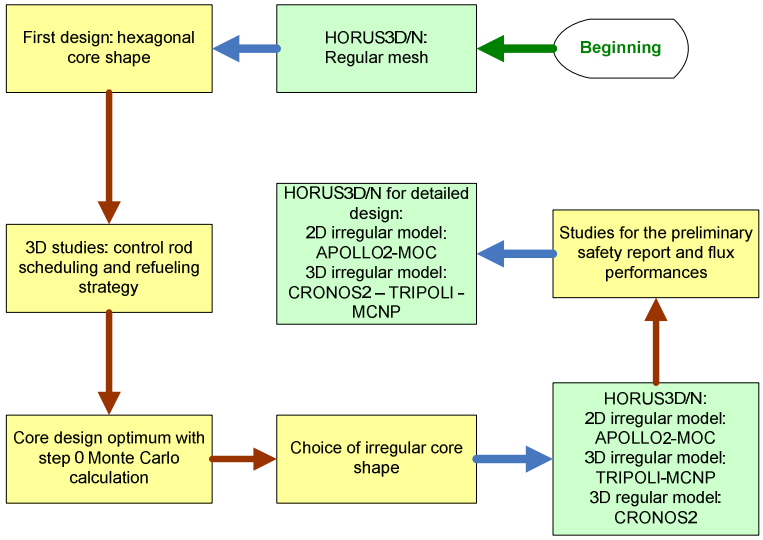

Then the CEA developed a new 2D calculation scheme included in HORUS3D/N V2 [2]. This scheme is based on APOLLO2/MOC [7] solver in general geometry, including interface capabilities with the 3D Monte Carlo TRIPOLI4 code [8].

After calculating the 3D burn up and depletion with APOLLO2/MOC models, the composition data are fed back into a TRIPOLI4 model. To deal with axial phenomenon, this scheme includes a CRONOS2 3D calculation of the nearest regular core.

The latest release of the HORUS3D/N V3.0 [13] contains APOLLO2 MOC 2D calculation scheme for fuel assembly and reflector in general geometry. It also contains major developments of a 3D calculation scheme based on CRONOS2 code including capabilities for irregular geometries.

Those schemes are combined with several pre and post-processing tools such as:
- SILENE[5] to generate mesh calculation for APOLLO2/MOC,
- Object-Oriented PYTHON modules [10] to couple calculation schemes with the SALOME platform[12] and CHARM[14]

Furthermore, reactor performances such as flux level in the experimental devices were also performed by a dedicated MCNP based model. Starting from a database, a FORTRAN tool converts MOC output libraries into MCNP material format and generates MCNP input files at each depletion step.

4. Second example: pre and post-processing tool CHARM

CHARM-V2 is a Pre Post Processor for APOLLO2/MOC, TRIPOLI4 and MCNP based on an Open Cascade technology [12]. The CHARM project is developed by AREVA NP in collaboration with an AREVA TA partnership to integrate small reactor modelling needs.

Currently, this tool is embedded in many projects dedicated to experimental reactor and naval propulsion. The main advantages of this tool are listed as follow:
- A multipurpose user friendly graphical interface to design geometry, meshes, material association, to configure score and tally and also to visualize results projected onto geometry,
- A common geometry for APOLLO2/MOC, TRIPOLI4 and MCNP,

- A suitable XML file format describing exactly a CHARM study which can be easily modified by a script for parametric studies, studies are also saved in HDF file format as for a SALOME study,
- A batch mode to automatically generate numerous input data.

CHARM has commonly been used to generate parametric geometries including more than 30,000 meshes.

JHR modelling

This tool has been used for modelling the Jules Horowitz Reactor (Figure 1).

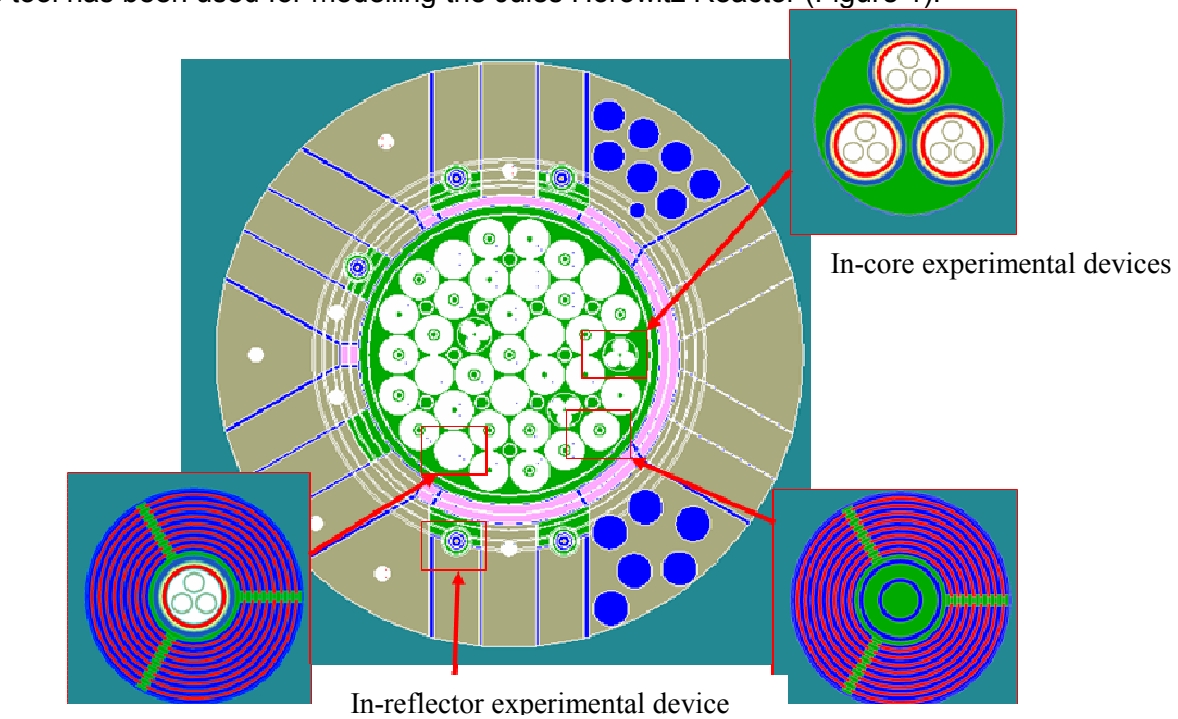

Figure 1: JHR modelling with GUI CHARM-V2

The making of a JHR input data with CHARM-V2 can be divided into two items:

- First the design of physics geometry,
- Then the configuration of mesh algorithms.

The main steps to model JHR are described below.

Step 1: Creation of the assemblies

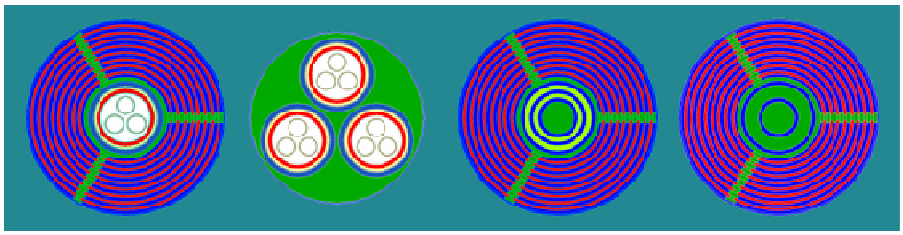

Figure 2: Modelling of different cores elements (isolated experimental device, experimental devices, fuel elements)

Step 2: Creation of the aluminium matrix,

Step 3: Introduction of fuel elements and experimental devices,

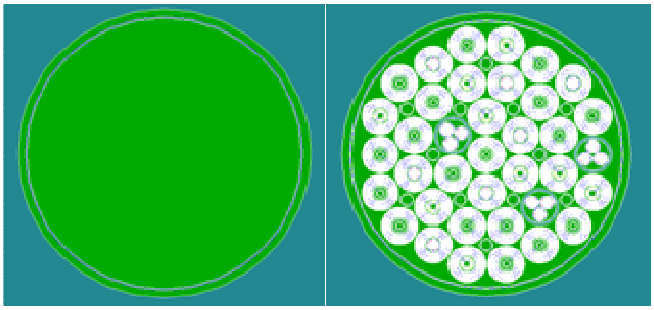

Figure 3 and 4: Modelling of aluminium matrix and full core

Step 4: Creation of void reflector and experimental cells. Creation of an overall reflector by an over draw with experimental cells,

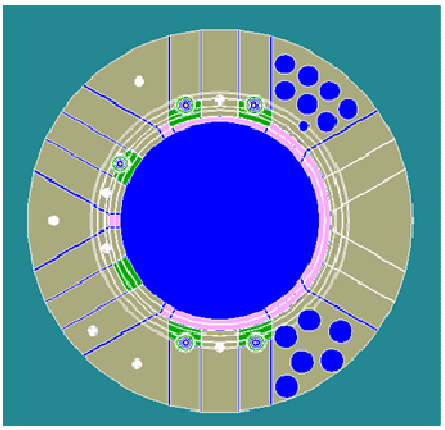

Figure 5: Modelling of complete reflector

Final step: Insertion of core and reflector to model the whole JHR (Figure 1).

Display results

In his stage of development, CHARM-V2 allows us to get give the mesh and geometry for the APOLLO2 MOC scheme.

Results obtained from these files are presented with the MED format of the SALOME [12] platform in figure 6.

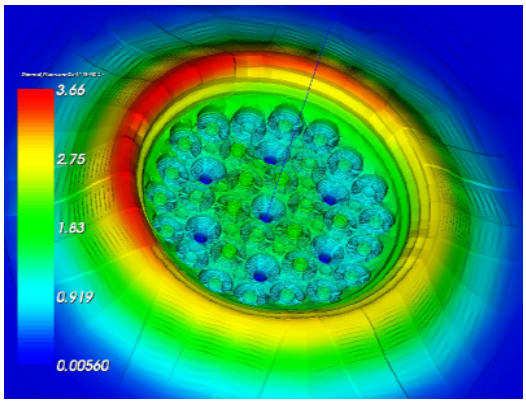

Figure 6: Visualization of the JHR thermal flux, APOLLO2-MOC

5. Third example: Monte Carlo burn up code

This example deals with a running project of material and test reactor design.

The objective is to design a MTR dedicated to scientists and operating teams of power reactor to come on. Several core configurations are studied. One of them fulfils the following conditions:

- Orthocylindric shape (68 cm x 68 cm),
- Fuel type: pin,
- Annular core with central and external reflector (graphite),
- With a key performance in thermal neutronic flux of 10^{13} n./cm^2/s in natural convection.

In the preliminary design study, AREVA TA have combined approaches:
- one uses a deterministic calculation scheme with APOLLO2-CRONOS2,
- the other uses a probabilistic calculation scheme based on MONTEBURNS [15] with MCNP [9]/ORIGEN [16] chained runs, and the pre-post treatment developed in the AREVA reactor framework,
- we are analyzing the results obtained by both methods with the depletion effect for the:
    - Possibilities for experimental devices,
    - Choice of the fuel type,
    - Fuel assembly design,
    - Core and reflector geometries.

As an illustration, some of the neutronic parameters for different cores (a, b, c) are listed below:
- Safety parameters: power peak,
- Thermal flux performances,
- Neutronics in operation: the example of reactivity during a standard week.

Power peak: The following figure shows a view of a core and the associated power map at step 0:

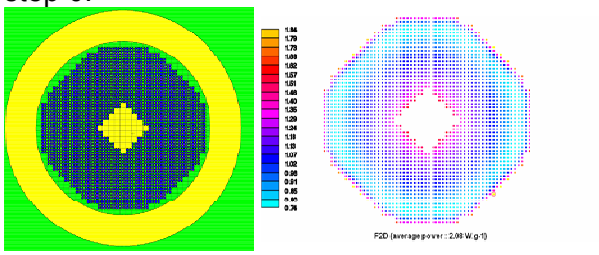

Figure 8: a-b cores

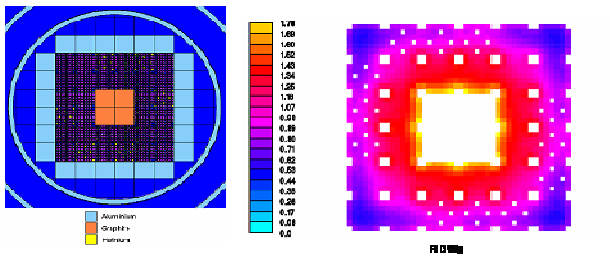

Figure 9: c core

The heat zone of the core is located around the central reflector, close to internal instrumentation (white areas in the right picture), which is due to thermalization peaks in water.

Thermal fluxes: This figure presents the evolution of the thermal fluxes in time, using Monteburns:

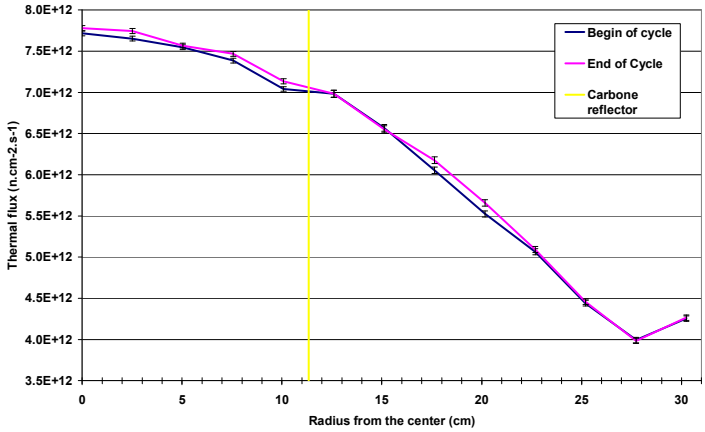

Figure 10: a-b cores – Thermal fluxes in evolution

As it can be seen on the figure below, the flux is slightly the same, in BOC (Beginning Of Cycle) and EOC (End Of Cycle) with a small increase with the irradiation, in order to compensate for vanishing U235.

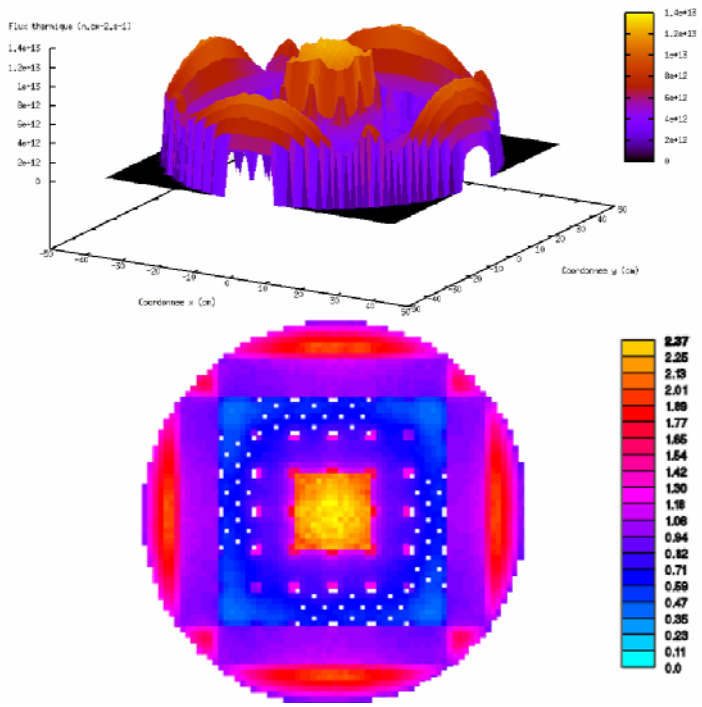

Figure 11: c core – Thermal fluxes at step 0 and associated heat map

The flux shape is as expected with the two reflector effects identified:
- An overflow in graphite reflector zone (left from yellow on figure 10),
- A rise on the outer core.

Example of reactivity during a standard week: This figure represents the xenon reactivity under the following operational conditions:
- 5 days a week (Monday to Friday),
- Half a day at full power,
- Then half a day: shutdown.

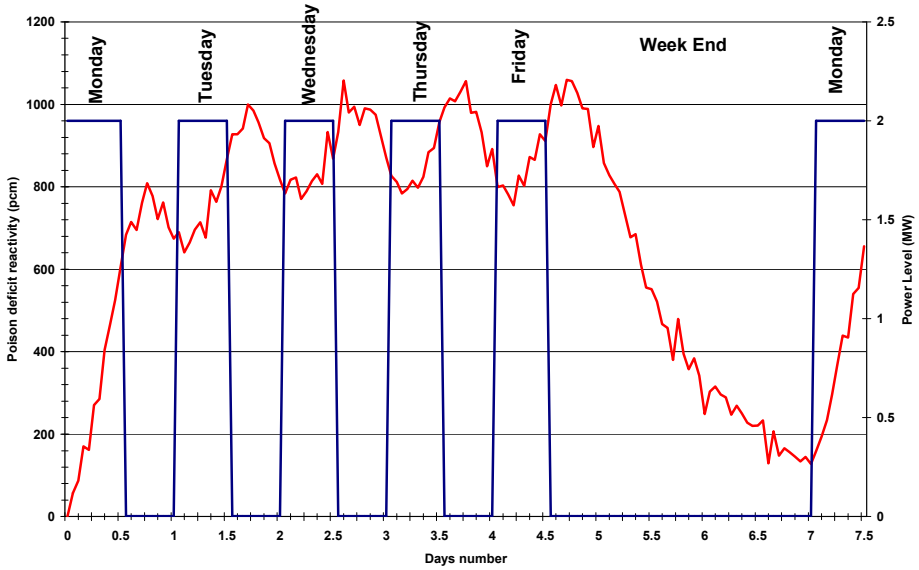

Figure 12: xenon reactivity in a standard week

So the capability of using such reactor switch on during the day (full power) and switch off during the night is highlighted as the Xenon peak has disappeared each time the reactor is switched on again.

6. Conclusion

AREVA TA carries out the design of the small reactor cores with both deterministic and probabilistic calculation schemes to improve the reached performances and safety analysis.

During these projects, benchmarks between the two schemes have been realized and have been demonstrated revealed good agreements for all neutronic common parameters.

The results of these benchmarks allow us to use both probabilistic and determinist codes for core design in a faster, more efficient and safer way.

7. Acknowledgments

AREVA NP for the CHARM development.
The CEA for TRIPOLI, APOLLO, CRONOS and the associated developments and reports.
Others members of AREVA TA neutronic teams:
- Of JHR project : L. Tillard, L. Manifacier, S. Czernecki, C. Edon, F. Attale (AREVA NP), S. Milesi, N. Bonhomme (AREVA NP)
- R&D project: J. Tixier, E. Duchemin.

8. References

1. G. Willermoz., V. Brun,, J. Di-Salvo, C. Döderlein: “New Developments for the Horowitz Reactor's neutronics modeling and validation”, PHYSOR 2002, Seoul, Corea.
2. N. Huot, A. Aggery, D. Blanchet, C. D'Aletto, J. Di Salvo, C. Döderlein, P. Sireta, and G. Willermoz: “The JHR neutronics calculation scheme based on characteristics method”, In Mathematics and Computation, Supercomputing, Reactor Physics and Nuclear ans Biological Applications, on CD-ROM, Avignon, France, sept 12-15 2005.
3. J.J. Lautard, S. Loubière, and C. Fedon-Magnaud: “CRONOS, a modular computational system for neutronic core calculations”, In IAEA topical meeting, Advanced calculational methods for power reactors, Cadarache, France, 1990.
4. S. Loubière, R. Sanchez, M. Coste, A. Hébert, Z. Stankovski, C. Van Der Gucht, and I. Zmijarevic: “Apollo2 Twelve Years Later”, In International Conference on Mathematics and Computation, Reactor Physics and Environmental Analysis in Nuclear Applications, volume 2, pages 1298_1315, Madrid, Espagne, September 27-30 1999.
5. Z. Stankovski: « La java de silène : A graphical user interface for 3d pre & post processing », In Joint International Conference on Mathematical Methods and Supercomputing for Nuclear Applications, Saratoga Springs, NY USA, October 6-10 1997.
6. G. Willermoz, A. Aggery, D. Blanchet, C. Chicoux, J. Di Salvo, C. Doderlein, D. Gallo, F. Gaudier, N. Huot, S. Loubière, and B. Noël: “Horus3D code package development and validation for the JHR modelling”, In Physor 2004, The Physics of Fuel Cycles and Advanced Nuclear Systems : Global Developments, on CD-ROM, Chicago, Illinois, april 25-29 2004.
7. A. Aggery, C. d'Aletto, J. Di Salvo, R. Sanchez, S. Santandrea, M. Soldevila, and G. Willermoz: “The characteristics method applied to a MTR whole core modelling”, In PHYSOR 2004 - The physics of Fuel Cycles and Advanced Nuclear Systems : Global Developements, on CD-ROM, Chicago, Illinois, april 25-29 2004.
8. J. Both, B. Morillon, and J. Nimal: “A survey of tripoli-4”, In 8th International Conference on Radiation Shielding, pages 373_380, Arlington, Etats-unis, april 24-27 1994.
9. J.F BRiesmeister: “MCNP- A General Monte Carlo N-Particle Transport Code”, Version 4C, LANL 13709-M, March 2000.
10. T. Bonaccorsi, J. Di Salvo, A. Aggery, C. D'aletto, C. Döderlein, P. Sireta, G. Willermoz, and M. Daniel: “Development of a multi-physics calculation platform dedicated to irradiation devices in a material testing reactor”, In Physor 2006 American Nuclear Society Topical Meeting on Advances in Nuclear Analysis and Simulation, on CD-ROM, Vancouver, Canada, September 10-14 2006.
11. Open Cascade: “Open cascade, simulation integrator”, http://www.opencascade.org/, 2009.
12. Open Cascade: “Salome : The open source integration platform for numerical simulation”, http: // www. salome-platform.org , 2007.
13. C. Döderlein, T. Bonaccorsi, C. D'Aletto, J. Di Salvo, O. Guéton, L. Lamoine, F. Moreau, G. Naudan, P. Siréta., “The 3D neutronics scheme for the development of the Jules-Horowitz-Reactor”, International Conference on the Physics of Reactors”, Interlaken, Switzerland, September 14-19, 2008
14. Charm: “Speed up the design of nuclear power plants using OPEN CASCADE software components”, http://www.opencascade.com/customers/successmain/areva_charm/
15. D.I Poston, H.R. Trellue: “User’s Manual Version 2.0 Monteburns”, September 1999, LA-UR-99-4999
16. A.G. Croff: “A user’s manual for the ORIGEN2 computer code”, ORNL/TM-7175, July 1980

RELAP ANALYSIS OF THE BR2 LOSS OF FLOW TEST A

C. P. TZANOS, B. DIONNE, J. MATOS
Nuclear Engineering, Argonne National Laboratory
Argonne, Illinois 60439

ABSTRACT

To support the conversion of the BR2 research reactor to low-enriched uranium (LEU) fuel and extend the validation basis of the RELAP code for the safety analysis of the conversion of research reactors from highly enriched (HEU) fuel to LEU, the simulation of a number of tests performed in 1963 at BR2 has been undertaken. These tests are characterized by loss of flow initiated at different reactor power levels with or without loss of pressure. This work presents the RELAP analysis of Test A/400/1 and comparison of code predictions with experimental measurements for peak cladding temperatures during the transient at different axial locations in an instrumented fuel assembly. The test simulations show that accurate representation of the pump coastdown characteristics, and of the power distribution, especially after reactor scram, between the fuel assemblies and the moderator/reflector regions are critical for the correct prediction of the peak cladding temperatures during the transient. Detailed MCNP and ORIGEN simulations were performed to compute the power distribution between the fuel assemblies and the moderator/reflector regions. With these distributions the agreement between computed and measured peak cladding temperatures is good.

Introduction

In 1963, a number of loss of flow tests were performed at the Belgian research reactor BR2 to demonstrate that the reactor can normally operate safely at the maximum heat flux of 400 W/cm^2, and to determine the maximum heat flux at which safe reactor operation can be maintained [1]. These tests are characterized by loss of flow initiated at different reactor power levels with or without loss of pressure. The A series of tests was performed at a maximum heat flux of 400 W/cm^2, and was initiated by a loss of flow followed by the opening of a by-pass valve that establishes a flow path connecting the cold and hot legs of the primary system. The series C and F of tests were performed at a maximum heat flux of 600 W/cm^2. Test C was the most severe test in terms of the peak cladding temperatures reached during the test, while test F was the most severe test in terms of safety limitations arising from coolant boiling. To support analyses to be performed with the RELAP code [2] for the safety analysis of the BR2 conversion from HEU fuel to LEU, it has been planned to analyze tests A, C, and F. These analyses will provide validation information for the use of RELAP in the BR2 analyses, as well as for other research reactors operating at conditions similar to those at BR2. This work presents the analysis of Test A/400/1 [3], which, for brevity, in this paper will be referred as Test A.

BR2 is a water-cooled thermal reactor moderated by water and beryllium. Normally, the coolant flows from the top of the core to the bottom. The beryllium moderator is a matrix of hexagonal prisms each having a central bore that contains either a fuel assembly, a control or regulating rod, an experimental device, or a beryllium plug. Each fuel assembly is composed of six concentric fuel plates divided by aluminum stiffeners into three sectors. The fuel is an Al-U alloy with uranium enriched 90% in U235. The cladding is aluminum. The main dimensions of the fuel plate are: active(fuel) length of 762 mm, active thickness of 0.5 mm, total thickness of 1.27 mm, and total length of 965 mm.

Cladding temperatures where measured on the outer surface of the outer plate (plate number six) of an instrumented assembly at five axial locations in the middle of one of the three sectors of this assembly. One of the thermocouples was located at the mid point from the bottom to the top of the active length, and the other thermocouples were placed at 150 and 300 mm above and below the mid point.

The RELAP Model

A RELAP5-3D model (RELAP5-3D, Version 2.4.2ie) was developed that is based on an original RELAP model provided by BR2 [4]. This RELAP5-3D model simulates the primary system loop, the reactor vessel, the components inside the vessel, the shroud cooling system and the reactor pool. The primary system is represented by one loop, one pump, and one heat exchanger. The pressurizer is represented by a time dependent volume that sets the pressure boundary condition. The shroud cooling system provides heat removal by circulating water in the gap between a shroud surrounding the reactor vessel and the reactor vessel. The flow paths inside the reactor vessel include: four channels for the instrumented assembly; one channel for the remaining fuel assemblies; one channel for the plugged assembly positions, the control rod flow paths, and the cooling path of the in-vessel irradiation (experiment) locations; and one channel for the by-pass flow (flow in the gap between assembly blocks, between assembly blocks and the reactor vessel, and through holes in beryllium blocks). Because the explicit simulation of each fuel plate in each sector of the assembly imposes a very long computation time, it was determined that it was adequate to split the instrumented assembly into four channels: three channels for a portion of the instrumented sector, and one for the remaining of the instrumented assembly. The three channels of the instrumented sector were: one for the gap between the sixth fuel plate (instrumented plate) and the Be block; one for the gap between the fifth and sixth plate, and one for the gap between the fifth and fourth plate.

Analysis and Results

The drivers of the Test A transient were [3]: shutting off the power to the main pumps at 5.35s from the time of test initiation; reactor scram on a loss of flow signal at 7.7 s; and opening of the bypass valve. This valve started to open at 22 s and was completely open at 35.6 s.

A set of pump homologous curves were provided by BR2, as well as a set of pump coastdown measurements (flow versus time)[3]. To improve the agreement between measured flow versus time and the flow predicted by the homologous curves, the pump friction torque was modified after 12 s and a valve was added in the primary system, which was closed after about 20 s at a rate that brought the predicted flow to a good agreement with the measured flow. The homologous curves with the modified pump friction torque and the added valve were used for the prediction of the flow during the Test A transient.

During Test A, the cladding temperature peaks immediately after the pump is shut off, then it comes down significantly as the reactor power drops, and then a second peak is reached around the time when the flow in the fuel channels reaches a zero value and then reverses. Simulations with a varying slope of the pump coastdown curve at the initiation of pump coastdown show that the first peak of the cladding temperature is sensitive to the value of this slope.

RELAP simulations of Test A had been performed at BR2 [4] using the decay heat curve of the ANS79-1 standard [5]. The predicted cladding temperature at the second peak was about 75°C higher than the measured temperature. Simulations at ANL produced quite similar results. In

research reactors, a significant fraction of the photons generated by radioactive material in the fuel plates are transported and absorbed in the moderator/reflector region. RELAP simulations using a rough estimate of the decay heat split between fuel plates and the moderator/reflector region gave a good agreement between predicted and measured peak cladding temperatures. Simulations with significant perturbations in the flow coastdown curve, the fuel channel heat transfer coefficient, and in the heat removed by the shroud cooling system had a minor impact on the predicted temperature for the second peak. Based on these results, MCNP and ORIGEN simulations were performed to determine the heat generation in the fuel and in the moderator/reflector regions after reactor scram. These simulations are discussed in Ref. 6. The power distributions determined in these simulations at steady state, as well as after reactor scram, were used in the final analysis of Test A.

In the original RELAP model provided by BR2, the instrumented assembly was represented by an average fuel plate, and five axial nodes where used in the active (fuelled) region of the fuel plate. Before proceeding to the final analysis, a number of sensitivity analyses were performed with the “average-plate” model and the above mentioned rough estimate of the decay heat split between fuel plates and the moderator/reflector region.

To assess the impact of the number of axial nodes on the predicted peak cladding temperatures, simulations where performed using five, ten and twenty axial nodes in the active region of the fuel plate. These simulations show that the predicted peak cladding temperature depends on the number of axial nodes, and increasing the number of axial nodes in the average fuel assembly did not affect the predicted peak cladding temperature in the instrumented assembly. Because the computation time increases with the number of axial nodes, in the following simulations twenty nodes where used in the active region of the fuel plates of the instrumented and average assembly. Assuming that the predicted peak cladding temperature would increase with the number of nodes (over twenty nodes) at the same rate as it increased from ten to twenty nodes (conservative assumption), then the predicted peak cladding temperature with a very large number of nodes would be about 3.3°C higher than that predicted by the twenty-node simulation. The sensitivity analyses also showed that the correction of the flow to match the measured flow coastdown, and the opening of the bypass valve had no significant effect on the predicted cladding temperature at the time of the second peak.

The results presented below are based on the power distributions determined from the MCNP and ORIGEN simulations of Ref. 6 mentioned earlier. Figure 1 shows measured and predicted temperatures for Test A at the locations of 300 mm (thermocouple TC11), 150 mm (thermocouple TC12), 0.0 mm (thermocouple TC13), and -150 mm (thermocouple TC14) from the mid-height of the active-fuel section of the instrumented plate. No measurements are available for Test A for the location of -300 mm. Table 1 summarizes the peak cladding temperatures at the location of each thermocouple and the time these peak values are reached from the initiation of the test. At steady state, the predicted peak cladding temperature for the instrumented plate is 6°C lower than the measured temperature. At the other thermocouple locations the difference between predicted cladding temperatures and measurements is smaller. The BR2 reference [3] for Test A states that the effective time of reactor shutdown was 7.5 s. The plots of the experimental data show that the first peak occurred a few fractions of a second earlier than the effective reactor shutdown time. This discrepancy may be due to uncertainties in data recording. The maximum discrepancy between measured cladding temperatures at the first peak and predicted temperatures is about 9°C. This is the temperature at the location of thermocouple TC13. The predicted peak cladding temperature of the instrumented plate (123.6°C, at the location of thermocouple TC14) is only 3.7°C higher than the measured temperature. As mentioned earlier, sensitivity analyses show that the predicted cladding temperature at the first peak is very sensitive to the slope of the pump coastdown curve

immediately after the pump is shut off. For example, for a linear pump coastdown curve that goes to zero in 2 s, the predicted peak cladding temperature (first peak) of the instrumented plate is 176°C.

The predicted time of the second peak in cladding temperatures is slightly longer than the measured time. The maximum discrepancy between predictions and measurements is 1.7 s. The predicted maximum cladding temperature at the time of the second peak, at the thermocouple locations, is 110.1°C. This is 1.4°C lower than the measured temperature (thermocouple TC14). The maximum discrepancy between predicted and measured temperatures at the time of the second peak is about 17°C at the location of thermocouple TC12. RELAP predicts that the maximum cladding temperature occurs about 19 mm above the location of thermocouple TC14, and is 0.8°C higher than that at the location of TC14.

The flow rate in the instrumented channel, reaches a zero value at 42.7 s, about 5 s later than the cladding temperature peaks in plate six, and then is reversed. During the time that the flow remains at near zero values the heat generated in the instrumented fuel plate is transferred to the beryllium block by local natural convection. The flow reverses very nearly at the time the coolant temperature reaches its maximum value at the bottom of the channel (bottom of active fuel).

In the channel between plates five and six, the flow reverses at 35.1 s from the initiation of the test. The temperature at the bottom of the channel reaches a maximum value at 35.0 s, and the cladding temperature peaks at 38.3 s, that is, 3.2 s after flow reversal. Around the time of flow reversal, this channel, which is bounded by two fuel plates, behaves differently than the instrumented channel, which is bounded by a fuel plate and a beryllium block that is colder than the coolant. Around the time of flow reversal, the natural circulation patterns in these channels (instrumented, and channel between plates) are different.

Summary and Conclusions

To support the safety analysis of the BR2 research reactor for conversion to LEU fuel and extend the validation basis of the RELAP code for the safety analysis of the conversion of other research reactors from HEU fuel to LEU, the BR2 Test A was analyzed with RELAP. During this test, the clad temperature peaks immediately after the pump is shut off. It comes down significantly as the reactor power drops, and a second peak is reached around the time when the flow in the fuel channels reaches a zero value and then is reversed. The RELAP simulations show that the value of the first peak is sensitive to the slope of the pump coastdown curve at the initiation of pump coastdown, while that of the second peak is sensitive to the power distribution between the fuel assemblies and the moderator/reflector regions. Test A simulations where performed with power distributions computed from detailed MCNP and ORIGEN analyses that provide the decay heat distribution between the fuel and moderator/reflector regions. With these distributions the agreement between computed and measured peak cladding temperatures is good.

At steady state, the maximum discrepancy between measured and predicted cladding temperatures is 6°C. At the first peak, the maximum discrepancy between measured and predicted cladding temperatures is 9°C, while this discrepancy for the peak cladding temperature of the instrumented plate is only 3.7°C. The maximum discrepancy between predictions and measurements for the time of the second peak in cladding temperatures is 1.7s. The predicted maximum cladding temperature at the time of the second peak is 1.4°C lower than the measured temperature. The maximum discrepancy between predicted and measured temperatures at the time of the second peak is 17°C.

References

1. G. Stiennon, et.al., “Experimental Study of Flow Inversion in the Belgium Reaction BR2,” Proceedings of the Third International Conference on the Peaceful Use of Atomic Energy, Geneva, 31 August – 9 September, 1964.
2. RELAP5-3D Code Development Team, “RELAP5-3D Code Manual,” INEEL-EXT-98-00834, 2005.
3. Data of Loss of Flow Tests Performed at BR2 in 1963, Personal Communication with Edgar Koonen of BR2, April 2009.
4. Personal Communication with Simone Heusdains of BR2, April 2009.
5. ANSI/ANS-5.1-1979, “Decay Heat Power in Light Water Reactors”, 1979.
6. B. Dionne, C. P. Tzanos, and J. Matos, “Detailed BR2 Steady State and Decay Power Distributions During 1963 A/400/1 Flow Test,” The 2009 International Meeting on Reduced Enrichment for Research and Test Reactors, Beijing, China, November 1-5, 2009.

Table 1. Peak Cladding Temperatures (°C) and Time (s)

	Steady State		First Peak				Second Peak			
	Measured	Predicted	Measured		Predicted		Measured		Predicted	
			Time	Temp	Time	Temp	Time	Temp	Time	Temp
TC11	41	41.5	7	42.2	7.5	43.2	41.4	81.1	41.7	69.5
TC12	53.8	54.4	7.3	54.3	7.5	59.2	39.7	95.8	40.5	79
TC13	89.5	91	7.3	95.2	7.5	104.3	37.9	113.5	39.1	100.9
TC14	113.1	107	7.2	119.9	7.5	123.6	36.2	111.5	37.9	110.1

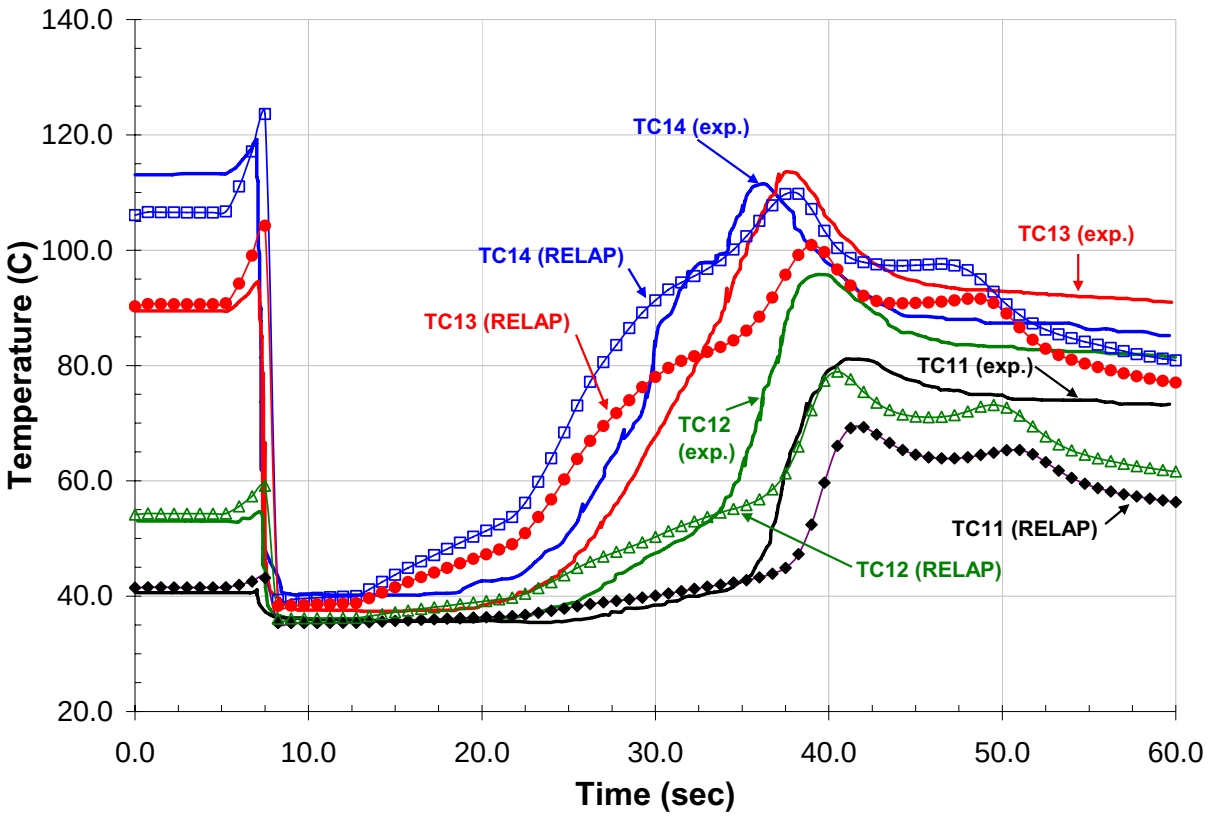

Figure 1. Measured and predicted cladding temperatures

European Nuclear Society

Rue Belliard 65, 1040 Brussels, Belgium
Telephone +32 2 505 30 54, Fax + 32 2 502 39 02
rrfm2010@euronuclear.org - www.euronuclear.org